Synergistic Effects of Microbial and Enzymatic Hydrolysis on the Growth Performance and Nutrient Utilization of BSF and Soybean in *Macrobrachium rosenbergii*: Mitigating Oxidative Stress and Enabling Metabolic Energy-Sparing

Karnchana Karnchanamayoon[1], Rungkan Klahan[2], Doungporn Amornlerdpison[1], Pairote Wongputtisin[3], Piyanuch Niamsup[2], Sudaporn Tongsiri[1]*

[1]Faculty of Fisheries Technology and Aquatic Resources, Maejo University, Chiang Mai, Thailand.
[2]Department of Aquaculture, Faculty of Agricultural Technology, Phetchaburi Rajabhat University, Phetchaburi, Thailand.
[3]Program in Biotechnology, Faculty of Science, Maejo University, Chiang Mai, Thailand.
*Corresponding Author Email: sudaporn@mju.ac.th

Abstract
The present study aimed to investigate the synergy effect of the use of BSF (*Hermetia illucens*) and SB (soybean) in combination as a fish meal and supplementing the feeding with microbial solid-state fermentation (MSF) using a co-inoculant of *Rhizopus microsporus* and *Lactobacillus reuteri* in feeding *Macrobrachium rosenbergii*. Sustainable BSF is limited by a tough, crystal-like alpha-chitin lattice responsible for damage to the structure of the intestine; SB harbors antinutritional properties causing systemic inflammation. The biological optimum was T6 (50% fermented BSF/SB and bromelain), which had the highest final weight (18.80 ± 1.26 g), specific growth rate (1.18 ± 0.17%/day), and feed conversion ratio (2.24 ± 0.30). FTIR spectra and SEM confirmed that fermentation was effective in reducing the chitinous matrix, resulting in an energy-sparing effect. This was manifested by a marked decrease in the endogenous secretion of protease from 6.88 ± 0.60 to 3.89 ± 0.14 mU/min/mg protein, with metabolic energy focused on somatic growth. However, the raw diets (T3 and T4) caused mechanical chitin abrasion and chemical irritations, which led to the highest level of MDA (3.18 ± 0.37μmol/g protein). T6 had the lowest oxidative stress (1.41 ± 0.04 μmol/g protein), and full replacement (T7) promoted metabolic overload and hyperlipidemia (73.53 ± 11.16 mg/dL triglycerides). In addition, fermentation promoted the integrity of the exoskeleton by generating prebiotic chito-oligosaccharides (maximum chitin yield 24.77 ± 2.15%). The results presented here confirm the potential of the 50% synergistic replacement approach, in combination with microbial and enzymatic bioprocessing, as a validated pathway for sustainable and efficient aquaculture.

Keywords: *Hermetia illucens*, Giant freshwater prawn, Solid-state fermentation, Bromelain, Digestive enzymes, Chito-oligosaccharides, Antioxidant capacity

1. Introduction

The giant freshwater prawn *Macrobrachium rosenbergii* is an important aquaculture species because of its rapid growth rate and high market demand (Sun et al., 2020; Valente et al., 2024). However, further scale-up of prawn production would rely, in part, on the reduction of marine fishmeal usage, which is expensive and whose prices fluctuate according to market dynamics, instead of using alternative proteins with efficient digestibility, higher amino acid content, and less damage to the environment (Gutiérrez-Pérez et al., 2022; Yohana et al., 2023). Meals derived from soybean (SB) and defatted black soldier fly (DBFS) are potential options owing to their nutrient composition and reproductive potential. However, some nutritional constraints may limit their use in the diets of decapods. In addition to the anti-nutritional factors present in soybeans that affect digestion, nutrient assimilation, and gut health (Peng et al., 2022), DBFS has a considerable chitin component with a highly ordered crystalline structure (Brigode et al., 2020; Mohan et al., 2022), which can hinder digestive enzymes from reaching the nutrients encapsulated in the beads. Therefore, high percentages of untreated plant- and insect-derived ingredients in the diet might adversely affect nutrient assimilation, break down intestinal homeostasis, cause oxidative stress, and affect growth performance (Moutinho et al., 2022).

To flank these limitations, bioprocessing strategies can be used to increase the nutritional and functional qualities of alternative feed ingredients. Selected microorganisms such as *Rhizopus microsporus* and *Lactobacillus reuteri* can partially be used to break down complex matrices of feeds, reduce the anti-nutritional compounds, and enhance the bioavailability of the nutrients through solid-state fermentation (Kalaiselvan et al., 2025; Barrera-León et al., 2025). Low molecular-weight peptides and bioactive metabolites due to fermentation could also contribute to the integrity of the gastrointestinal tract and the health of the host. However, total protein hydrolysis cannot be guaranteed with microbial fermentation without additional processes. The use of an exogenous protease may therefore be an extra pathway to enhance protein digestion and nutrient utilization.

Bromelain is a wide-acting protein-cleaving enzyme, which is a broad-spectrum cysteine protease that cleaves a variety of dietary proteins. To prevent the thermal denaturation process during feed processing, the bromelain in the present study was applied by spray coating after the extrusion process. It is hoped that the microbial

fermentation, together with the addition of Bromelain, will act as a two-step pre-digestion, with fermentation changing the structure and anti-nutritional nature of the feed matrix, followed by protein digestion in the digestive tract, facilitated by the presence of Bromelain. This results in the generation of peptides and amino acids, which are more readily absorbed and result in a decreased physiological need for the production of digestive enzymes. This energy-saving effect could free up a higher percentage of dietary energy and nutrients for tissue deposition and somatic growth (Blasco et al., 2021).

While studies have been conducted on the individual effects of plant and insect meals in aquafeeds, there is a lack of data on the simultaneous use of multi-strain fermentation and exogenous proteases in *M. rosenbergii* feeds. It is not yet known if all of these additional measures can be used together to allow them to affect both growth and digestive efficiency in combination with antioxidant capacity, immune competence, and nutrient retention. Better nutrient assimilation might also help to limit the output of nitrogenous and organic wastes to water, which could improve water quality. Furthermore, given the relationship between mineral and nutrient metabolism with molting and exoskeletal development in crustaceans, the influence of these diets on the development of cuticular biomineralization needs to be explored.

Hence, the effects of fermented DBFS–SB blends and of bromelain supplementation on the growth performance, feed utilization, oxidative status, immunity, intestinal health and cuticular calcification of *M. rosenbergii* were assessed individually and synergistically. Dietary utilization will be investigated, along with changes to the water quality in the culture system, to see if the utilization can be improved to lower nutrient discharge. It is hoped that the results will shed light on the mechanism of this dual bioprocessing and prove the feasibility of developing sustainable feeds that are high in performance for freshwater prawn culture.

2. Methodology

2.1 Ethics Statement

All experiments on animal subjects were performed in accordance with the general guidelines for handling aquatic animals. The study protocol was approved by the Animal Ethics Committee for Experiments on Animals of Maejo University, Thailand, and it abides by the rules of the Institute of Animals for Scientific Purposes Development.

2.2 Experimental Animals and Design

The juvenile giant freshwater prawns, *Macrobrachium rosenbergii*, weighing at around 10 g, were purchased from a commercial hatchery in Thailand. The prawns were placed in 0.25 m2 plastic tanks for 7 days prior to the start of the trial, while being fed the control diet 5 times a day. The prawns were randomly stocked in each experimental tank at a population density of 15 prawns/tank after acclimation. The experiment was designed in a completely randomized block design consisting of seven dietary treatments and five replicates. The feeding trial was carried out for 60 days under a controlled environment.

2.3 Preparation of Fermented Substrates and Microbial Inoculants

2.3.1 Raw Material Sourcing

Dried soybeans with the hulls removed (*Glycine max* cv. dehulled). The commercial sources were commercial suppliers of Chiang Mai 60 and defatted black soldier fly (DBSF, *Hermetia illucens*) in Thailand. All raw materials were stored at temperatures below 10 °C at the same time in hermetically sealed plastic bags to ensure nutritional integrity.

2.3.2 Microbial Inoculants

Inoculants used for fermentation were *Rhizopus microsporus* and *Lactobacillus reuteri,* which were provided by the Agro-Industrial Biotechnology Laboratory, Faculty of Science, Maejo University. The fungal culture (*R. microsporus*) was grown at room temperature in potato dextrose broth. The spores were collected and resuspended in sterile 0.85% (w/v) NaCl solution for the desired concentration. The bacterial culture (*L. reuteri*) was grown in de Man, Rogosa and Sharpe broth at 30 °C. The biomass was removed by centrifugation and re-suspended in sterile 0.85% (w/v) NaCl to form the working cell suspension.

2.3.3 Solid-State Fermentation Process

Soybean preparation process, including the dehulled soya bean, was soaked in tap water for 6 h at room temperature, drained, and sterilized by autoclaving (121 °C, 15 psi) for 20 min. To prepare DBSF powder, it was rehydrated with distilled water (1 kg:1 L ratio), homogenized, and permitted to rehydrate for 30 min prior to the same sterilization process. Both substrates were co-inoculated with 10^8 spores/kg of *R. microsporus* and 10^8 CFU/kg of *L. reuteri* after cooling. The fermentation processes were carried out in stainless steel trays (30 cm × 100 cm) at a temperature of 25 °C under semi-aseptic conditions. Fermentation periods were optimized to be 24 h and 48 h for Microbial Hydrolyzed Soybean (MHSB) and Microbial Hydrolyzed Black Soldier Fly (MHFBSF), respectively. Hot-air drying at 80 °C until a constant weight was achieved stopped the process.

2.4 Enzyme Extraction and Activity Assays

2.4.1 Bromelain Preparation

The peels and cores of "Batavia" pineapples (Ananas comosus L.) from Lampang, Thailand, were used as the material for the bromelain extraction. The substrates were washed, finely minced, and homogenized using ice-cold distilled water 0.5:1 (w/v) for 5 minutes. This homogenate was filtered through muslin cloth and then centrifuged at 12000 rpm for 20 minutes at 4 °C. The collected supernatant was kept at 4 °C for experimental diet formulation and enzymatic analysis. The enzyme activity of total bromelain was determined based on the method of Ketnawa et al. (2012).

2.4.2 Digestive Enzyme Assays

The hepatopancreas of *M. rosenbergii* was used to extract digestive enzymes (protease, amylase, and lipase) according to the method described by Giménez et al. (2000). Protease activity was determined through the use of azo-casein as the substrate and by following the method described by Bezerra et al. (2005). Soluble starch was used as a substrate, and the amylase activity was determined according to the method described by Hashim et al. (2005). Lipase activity was determined by measuring the hydrolysis of p-nitrophenyl palmitate according to Markweg-Hanke et al. (1995).

2.5 Experimental Diets

Seven isonitrogenous and isolipidic experimental diets were formulated to systematically evaluate the physiological effects of black soldier fly larvae and soybean meal inclusion, microbial hydrolysis, and bromelain supplementation. The diets were designed to maintain comparable crude protein levels, ranging from 32.31 ± 0.18% to 33.20 ± 0.21%, and ether extract levels, ranging from 12.73 ± 0.16% to 14.38 ± 0.08%. The dietary treatments followed a progressive substitution strategy.

T1 served as the control diet and contained traditional fish meal (FM; 24%) and dehulled soybean (SB; 24.5%) without bromelain supplementation, while T2 consisted of the same basal diet spray-coated with bromelain at 250 ppt to isolate the effect of enzymatic supplementation. In T3, 50% of the fish meal was replaced with dried black soldier fly larvae (DBSF; 12% FM and 12% DBSF), whereas T4 involved complete replacement of fish meal with DBSF (0% FM and 24% DBSF), with both diets supplemented with 250 ppt bromelain. T5 contained conventional fish meal (24%) combined with microbially hydrolyzed soybean (MHSB; 32.5%) and 250 ppt bromelain. In T6, 50% of fish meal was replaced with microbially hydrolyzed black soldier fly larvae (MHBSF; 12% FM and 12% MHBSF) together with MHSB (32.5%) and 250 ppt bromelain, while T7 represented complete fish meal replacement using MHBSF (24%) and MHSB (32.5%), also supplemented with 250 ppt bromelain.

All experimental diets were processed into pellets using a single-screw extruder from Siam Farm Services Co., Ltd., Thailand. The bromelain supplementation level of 250 ppt was selected based on its previously demonstrated efficacy in improving growth performance, feed utilization, and intestinal morphology in *Litopenaeus vannamei* (Klahan et al., 2023).

2.6 Chemical Analysis

The proximate composition of the experimental diets was determined according to the official method of the Association of Official Analytical Chemists. Amino acid and fatty acid profiles were analyzed by the Central Laboratory Co., Ltd., with special in-house methods. The amount of amino acids was determined by method TE-CH-372, consistent with Commission Directive 98/64/EC. The fatty acid profiles were analyzed using method TE-CH-208, which is based on the standard method AOAC 996.06.

2.7 Rearing Environment and Physicochemical Monitoring

M. rosenbergii post-larvae were acclimated to the experimental conditions for a certain amount of time, and then were randomly distributed within the culture tanks. Five replications were used for each of the seven dietary treatments. The growth trial involved continuous monitoring and maintenance of physicochemical water quality parameters such as temperature, pH, dissolved oxygen, nitrogenous compounds (ammonia and nitrite), and minerals necessary for the species, throughout the growth period.

2.8 Hemolymph Extraction and Biochemical Assays

Hemolymph was collected from the prawns from the ventral sinus by using chilled 1 mL syringe at the end of the trial. The circulating total protein was determined by spectrophotometric measurement, and the level of glucose and triglyceride in the hemolymph was measured by an automated biochemical analyzer after allowing the samples to clot for 1 h at 4 °C and centrifuging at 4,000 × g for 10 min at 4 °C. Further, activities of malondialdehyde (MDA; E-BC-K025-M), catalase (CAT; E-BC-K031-M) and total superoxide dismutase (T-SOD; E-BC-K020-M) were measured using commercial kits (Elabscience Biotechnology, Inc., China) in accordance with the manufacturer's instructions, to evaluate the antioxidant status of the prawns.

2.9 Chitin Extraction and Quantification

The carapaces of *M. rosenbergii* were chemically demineralized and deproteinized following Maschmeyer et al. (2020) to extract and quantify chitin. To remove moisture from the carapace, the sample was dried at 60 °C for 24 h, and then finely homogenized to a powder. To remove the inorganic mineral part, 1 g of the ground sample was treated with 20 mL of 1 M HCl and stirred at room temperature for 2 h during the demineralization phase. The residue obtained was filtered and washed several times with distilled water until its pH became neutral.

In the deproteinization step, the mineral-free residue was subjected to the treatment of 20 mL of 1 M NaOH at 90 °C for 2 h to remove the associated proteins. After a reaction, the crude chitin was filtered, washed to a neutral pH, and dried at 60 °C until reaching constant weight. The chitin content was gravimetrically determined as final/initial dry weight and expressed as a percentage as follows:

$$Chitincontent(\%) = (\frac{W_{final}}{W_{initial}}) \times 100$$

where $W_{initial}$ represents the weight of the initial dry sample, and W_{final} the weight of the extracted chitin.

2.10 Structural and Morphological Characterization

The structural properties of chitin obtained from raw materials and prawn shells under various feeding treatments were analyzed using Fourier-transform infrared (FTIR) spectroscopy with the PerkinElmer spectrum Two spectrometer to identify structural functional groups. High-resolution Scanning Electron Microscopy (SEM; Tescan CLARA) was also used to analyze the surface topography of dietary chitin, the integrity of the carapace in *M. rosenbergii*, and the intestinal histology.

2.11 Data Collection and Growth Analysis

Prawns were weighed individually (to 0.01 g) every 30 days over the 60-day period during the trial. Water quality parameters were measured weekly, which were pH, temperature, nitrite, ammonia, alkalinity, calcium, and magnesium. The following formula was used to calculate the growth performance and feed utilization:

- Weight gain = $W_{final} - W_{initial}$
- Average daily gain = $\frac{W_{final} - W_{initial}}{days}$
- Specific growth rate = $\frac{100 \times ln(W_{final}/W_{initial})}{days}$
- Survival rate = $\frac{N_{final}}{N_{initial}} \times 100$
- Feed intake = $\frac{totalfeedconsumed}{initialnumberofprawns}$
- Feed conversion ratio = $\frac{totalfeedconsumed}{totalweightgain}$

where $W_{initial}$ *and* W_{final} *= initial and final weights;* $N_{initial}$ *and* N_{final} *= initial and final prawn counts;* t *= 60 days.*

One-way ANOVA was used to analyze all data (Mean ± SD). Duncan's Multiple Range Test was used to determine significant differences between treatment means at a 5% level of significance.

3. Results

3.1 Validation of Environmental Stability

Reliability of in vivo aquaculture trials depends on the existence of a stable rearing environment (Arbon et al., 2023). The physicochemical water quality parameters were significantly altered at 60-day end of the trial; no significant difference was observed between the seven dietary treatments ($p>0.05$). This consistency provides the basis for attributing any growth and physiological differences observed to the nutritional interventions, as much as possible.

The pH of water stays in the optimal mildly alkaline range throughout the experimental period with slight fluctuation between 8.24 ± 0.13 and 8.53 ± 0.63. Nitrogenous compounds were also kept within safe physiological limits of *M. rosenbergii* (Hittinahalli et al., 2023), such as nitrite level (1.66 ± 0.31 mg/L to 2.40 ± 0.35 mg/L) and ammonia level (1.76 ± 0.47 mg/L to 2.57 ± 0.47 mg/L). Moreover, essential minerals and buffering capacity remained relatively constant with mean values of 81.50 ± 7.04 to 91.25 ± 5.30 mg/L for alkalinity, and no significant changes were observed in the calcium and magnesium levels throughout the study.

Table 1: Physicochemical Water Quality Parameters across Experimental Treatments

Treatments	Water Quality Parameters						
	pH	Temperature (°C)	Nitrite (mg/L)	Ammonia (mg/L)	Alkalinity (mg/L)	Calcium (mg/L)	Magnesium (mg/L)
T1	8.26 ± 0.08	24.28 ± 0.26	1.86 ± 0.79	1.80 ± 0.41	81.75 ± 3.38	152.57 ± 20.06	13.60 ± 8.65
T2	8.53 ± 0.63	24.27 ± 0.22	2.29 ± 0.68	2.09 ± 0.70	87.50 ± 5.80	158.86 ± 22.73	18.15 ± 1.92
T3	8.24 ± 0.13	24.33 ± 0.29	1.85 ± 0.52	2.22 ± 0.14	81.50 ± 7.04	161.71 ± 23.96	16.98 ± 6.70
T4	8.28 ± 0.06	24.21 ± 0.12	2.18 ± 0.50	1.76 ± 0.47	85.50 ± 7.53	153.71 ± 29.17	14.89 ± 5.01
T5	8.27 ± 0.06	24.24 ± 0.19	2.20 ± 0.58	2.25 ± 0.87	91.25 ± 5.30	146.29 ± 7.11	13.43 ± 2.53
T6	8.28 ± 0.05	24.21 ± 0.14	2.40 ± 0.35	2.26 ± 0.73	90.75 ± 6.77	163.43 ± 26.53	12.37 ± 7.95
T7	8.28 ± 0.02	24.19 ± 0.09	1.66 ± 0.31	2.57 ± 0.47	89.75 ± 10.29	148.00 ± 10.38	10.66 ± 3.75

Note: Values are expressed as Mean ± SD ($n = 5$). No significant differences were observed among treatments ($p > 0.05$).

3.2 Proximate Composition of Raw Materials and Experimental Diets

The nutritional changes in the raw ingredients due to the fermentation bioprocess were explained by measuring the proximate compositions before diets were formulated. The crude protein content of the soybean meal was significantly higher after microbial co-fermentation (47.16 ± 0.51%) than with the use of soybeans alone (37.74 ± 0.26%) ($p<0.05$). This enrichment is presumably due to the conversion of carbohydrates and fibres into microbial single-cell protein (Yan et al., 2025). On the other hand, the extract concentration of DBSF decreased

significantly to that of MHBSF, 13.17 ± 0.45% to 10.58 ± 0.24%, indicating that the lipids in the feed were utilized as a major source of carbon and energy by the microbial consortium during the bioprocess (Table 2).

Table 2: Proximate Composition of Raw Materials (%)

Materials	Chemical composition (%)				
	Moisture	Crude Protein	Ether Extract	Crude Fiber	Ash
DBSF	7.80 ± 0.01 [a]	55.94 ± 0.13 [d]	13.17 ± 0.45 [b]	7.18 ± 0.20 [c]	8.57 ± 0.01 [c]
MHBSF	8.01 ± 0.01 [b]	53.06 ± 0.29 [c]	10.58 ± 0.24 [a]	7.10 ± 0.08 [c]	9.02 ± 0.01 [d]
SB	9.43 ± 0.04 [c]	37.74 ± 0.26 [a]	19.24 ± 0.06 [d]	2.72 ± 0.25 [a]	4.70 ± 0.04 [b]
MHSB	7.82 ± 0.02 [a]	47.16 ± 0.51 [b]	17.53 ± 0.15 [c]	3.45 ± 0.22 [b]	3.62 ± 0.02 [a]

Note: Values (Mean ± SD) within a column with distinct superscripts differ significantly ($p < 0.05$).

Table 3: Dietary and Proximate Composition of Experimental Diets (%)

Ingredients	Diets (kg)						
	T1	T2	T3	T4	T5	T6	T7
Fish meal	24	24	12		24	12	
Defatted BSF			12	24			
Dehulled Soy bean	24.5	24.5	24.5	24.5			
MHBSF[1]						12	24
MHSB[2]					32.5	32.5	32.5
Wheat Gluten	10	10	10	10	2	2	2
Wheat flour	7.5	7.5	7.5	7.5	7.5	7.5	7.5
Tapioca Starch	18	18	18	18	18	18	18
Dried Squid viscera meal	3	3	3	3	3	3	3
Dicalcium phosphate	2.5	2.5	2.5	2.5	2.5	2.5	2.5
Lecithin	1	1	1	1	1	1	1
DL-methionine	1	1	1	1	1	1	1
Premix	1.5	1.5	1.5	1.5	1.5	1.5	1.5
Soybean oil	2	2	2	2	2	2	2
Fish oil	3	3	3	3	3	3	3
Binder	2	2	2	2	2	2	2
Total (KG)	100	100	100	100	100	100	100
Bromelain (ppt)		250	250	250	250	250	250
Chemical composition (%)							
Moisture	7.98 ± 0.02 [f]	7.86 ± 0.01 [e]	6.15 ± 0.01 [a]	7.75 ± 0.02 [d]	7.77 ± 0.02 [d]	7.71 ± 0.01 [c]	7.64 ± 0.02 [b]
Crude Protein	32.59 ± 0.27 [a]	32.52 ± 0.16 [a]	33.20 ± 0.21 [b]	33.20 ± 0.11 [b]	32.65 ± 0.23 [a]	32.42 ± 0.10 [a]	32.31 ± 0.18 [a]
Ether Extract	13.42 ± 0.06 [b]	12.73 ± 0.16 [a]	12.80 ± 0.10 [a]	13.38 ± 0.10 [b]	14.38 ± 0.08 [e]	14.03 ± 0.13 [d]	13.79 ± 0.12 [c]
Crude Fiber	0.46 ± 0.13 [a]	0.35 ± 0.04 [a]	0.86 ± 0.11 [b]	1.78 ± 0.12 [d]	1.28 ± 0.04 [c]	1.68 ± 0.04 [d]	2.26 ± 0.03 [e]
Ash	8.69 ± 0.03 [e]	8.75 ± 0.00 [e]	8.62 ± 0.01 [d]	7.18 ± 0.02 [a]	8.87 ± 0.02 [f]	8.11 ± 0.10 [c]	7.36 ± 0.02 [b]

Note: Values within a given row designated by distinct superscripts differ significantly ($p < 0.05$).
[1]MHBSF - Microbial Hydrolyzed BSF
[2]MHSB - Microbial Hydrolyzed Soybean

Table 4: Amino Acid Profile

Amino Acid Profile	DBSF	MHBSF	SB	MHSB	T1	T2	T3	T4	T5	T6	T7
Essential Amino Acids (EAAs)											
Arginine	2601.05	2463.41	2730.42	2697.45	1677.81	1638.69	1726.13	1636.80	1768.75	1321.23	1608.60

Histidine	1700.46	1536.46	1073.14	1161.49	730.44	716.76	808.31	863.84	791.12	599.99	820.74
Isoleucine	2281.56	2262.38	1695.04	2066.03	1222.49	1208.31	1271.55	1291.92	1300.26	1039.36	1355.71
Leucine	3589.28	3541.74	2850.18	3344.82	2201.39	2172.18	2276.37	2286.04	2266.46	1789.41	2288.41
Lysine	3384.58	3213.67	2358.34	2472.85	1484.11	1436.22	1521.53	1486.37	1669.43	1278.33	1586.47
Methionine	1061.22	1144.19	555.66	610.00	1504.85	1461.82	1627.33	1593.98	1538.87	1600.02	1548.23
Phenylalanine	2167.54	2182.76	1988.53	2243.48	1466.65	1424.38	1535.20	1506.49	1447.09	1165.27	1514.92
Threonine	2213.22	2182.14	1537.22	1728.77	1141.46	1131.11	1189.38	1193.52	1223.84	956.61	1211.90
Tryptophan	662.98	569.93	435.88	518.51	247.19	237.55	270.89	281.16	275.90	290.97	286.31
Valine	3032.86	2865.84	1838.56	2187.28	1466.32	1424.71	1540.65	1627.56	1558.03	1254.79	1639.04
Non-Essential Amino Acids (NEAAs)											
Alanine	3380.14	2798.98	1641.70	2125.08	1547.02	1512.43	1608.62	1628.34	1713.74	1309.21	1584.94
Aspartic acid	5771.30	5640.59	4598.02	5217.41	2744.12	2719.10	2864.89	2939.63	3187.43	2516.61	3168.26
Cystine	502.84	460.81	603.81	599.64	434.98	432.01	455.90	454.64	367.58	370.51	338.97
Glutamic acid	5484.19	5139.40	6971.10	7600.65	6810.99	5766.85	6951.78	6797.62	5229.23	4254.06	5236.45
Glycine	2492.54	2466.99	1553.21	1769.72	1684.79	1651.36	1671.66	1543.22	1721.98	1323.18	1539.81
Hydroxylysine											
Hydroxyproline					<500.00	<500.00	<500.00		<500.00		
Proline	2764.70	2515.51	1841.93	2032.00	2164.01	2149.20	2358.41	2297.06	1843.16	1399.17	1972.60
Serine	2218.31	2099.24	1978.03	2197.68	1440.44	1426.64	1512.47	1539.69	1459.70	1126.75	1458.62
Tyrosine	3642.46	3275.19	1277.49	1515.63	919.82	926.88	1114.74	1376.38	1061.31	899.57	1292.73

Table 5 Fatty Acid Composition

Fatty acid composition	DBSF	MHBSF	SB	MHSB	T1	T2	T3	T4	T5	T6	T7
Butyric acid (C4:0)											
Caproic acid (C6:0)		0.01	0.03	0.04	0.02	0.03	0.02	0.02	0.01	0.01	0.02
Caprylic acid (C8:0)			0.09	0.07			0.01	0.01	0.02	0.02	0.02
Capric acid (C10:0)	0.12	0.08					0.01	0.02			0.02
Undecanoic acid (C11:0)											
Lauric acid (C12:0)	4.51	4.00	0.01	0.03	0.08	0.15	0.37	0.83	0.26	0.40	0.77
Tridecanoic acid (C13:0)											
Myristic acid (C14:0)	0.94	0.93	0.03	0.03	0.25	0.37	0.33	0.35	0.33	0.34	0.39
Pentadecanoic acid (C15:0)	0.05	0.05		0.01	0.04	0.06	0.05	0.04	0.06	0.05	0.05
Palmitic acid (C16:0)	2.26	2.32	3.87	4.50	2.30	3.44	3.05	2.73	3.68	3.46	3.50
Heptadecanoic acid (C17:0)	0.06	0.06	0.07	0.07	0.07	0.10	0.08	0.06	0.10	0.09	0.08

Stearic acid (C18:0)	0.56	0.58	1.34	1.93	0.73	1.08	0.95	0.80	1.49	1.28	1.13
Arachidic acid (C20:0)	0.04	0.04	0.10	0.15	0.05	0.08	0.07	0.06	0.10	0.09	0.08
Heneicosanoic acid (C21:0)			0.01	0.03	0.02	0.01	0.01	0.01	0.02	0.02	0.01
Behenic acid (C22:0)			0.15				0.08	0.07	0.10	0.09	0.09
Tricosanoic acid (C23:0)			0.03	0.03	0.01	0.02	0.02		0.02	0.02	0.02
Lignoceric acid (C24:0)			0.02	0.02			0.02	0.02		0.01	0.01
Saturated fat	8.56	8.12	5.76	6.94	3.58	5.38	5.08	5.02	6.21	5.90	6.21
Myristoleic acid (C14:1)	0.01					0.01			0.01	0.01	0.01
cis-10-Pentadecenoic acid (C15:1n10)											
Palmitoleic acid (C16:1n7)	0.28	0.19	0.02	0.03	0.24	0.36	0.22	0.15	0.32	0.28	0.22
cis-10-Heptadecenoic acid (C17:1n10)											

Table 5 (continued) Fatty Acid Composition

Fatty acid composition	DBSF	MHBSF	SB	MHSB	T1	T2	T3	T4	T5	T6	T7
Trans-9-Elaidic acid (C18:1n9t)	0.06	0.02		0.02	0.03	0.05	0.04	0.03	0.02	0.05	0.05
cis-9-Oleic acid (C18:1n9c)	2.48	1.68	5.29	6.46	2.15	3.32	2.37	2.00	3.82	3.53	3.25
cis-11-Eicosenoic acid (C20:1n11)	0.16		0.66	0.26	0.06	0.09	0.03	0.01	0.14	0.08	0.04
Erucic acid (C22:1n9)					0.03	0.02	0.01	0.01	0.02		0.05
Nervonic acid (C24:1n9)					0.02	0.02	0.02		0.02	0.01	0.01
Monounsaturated fatty acid	3.00	1.91	5.98	6.78	2.54	3.89	2.70	2.23	4.36	3.97	3.63
trans-Linolelaidic acid (C18:2n6t)						0.01			0.01	0.01	
cis-9,12-Linoleic acid (C18:2n6)	1.94	0.23	8.59	5.58	0.57	1.09	0.42	0.20	2.51	1.67	0.89
gamma-Linolenic acid (C18:3n6)				0.03							
alpha-Linolenic acid (C18:3n3)			0.04	0.06	0.06	0.08	0.05	0.04	0.08	0.07	0.06
cis-11,14-Eicosadienoic acid (C20:2)			0.02	0.02	0.01	0.02	0.02		0.03	0.02	0.02
cis-8,11,14-Eicosatrienoic acid (C20:3n6)	0.02	0.03	0.13	0.22	0.07	0.09					
cis-11,14,17-Eicosatrienoic acid (C20:3n3)			0.01		0.01	0.02			0.01		

Arachidonic acid (C20:4n6)			0.03	0.03		0.03	0.03	0.02	0.02	0.02	0.02
cis-13,16-Docosadienoic acid (C22:2)											0.02
cis-5,8,11,14,17-Eicosapentaenoic acid (C20:5n3)			0.09	0.17	0.04	0.06	0.06	0.05	0.07	0.07	0.07
4,7,10,13,16,19-Docosahexaenoic acid (C22:6n3)			0.02	0.01		0.01		0.01	0.01		0.01
Polyunsaturated Fatty acid	2.00	0.31	8.93	6.13	0.79	1.43	0.62	0.37	2.76	1.90	1.12
Unsaturated fat	5.00	2.21	14.91	12.91	3.34	5.31	3.32	2.59	7.12	5.87	4.75
Trans fat	0.06	0.03		0.02	0.04	0.06	0.05	0.04	0.04	0.06	0.06
Omega 3 (mg/100g)	19.88	21.46	157.04	244.41	124.68	171.16	133.14	113.06	169.49	161.20	157.90
Omega 6 (mg/100g)	1968.19	271.68	8754.78	5863.63	647.03	1215.15	459.14	229.20	2545.22	1699.19	908.77
Omega 9 (mg/100g)	2487.49	1682.66	5285.77	6467.21	2198.75	3366.82	2402.93	2023.31	3857.38	3548.04	3304.95

The formulated experimental diets were able to be successfully maintained at an isonitrogenous basis between 32.31% and 33.20% crude protein. The statistical analysis showed that the protein level was not different among the treatments, but was different for crude fiber ($p<0.05$). The diets with 100% FMR using insect meal (T4 and T7) had the highest fibre content of 1.78 ± 0.12% and 2.26 ± 0.03% respectively. The biochemical evidence of the substantial amount of chitin that the insects have injected into the feed matrix is the high amount of fibre in the feed matrix (Zainab-L et al., 2022). In addition, the difference in physiological responses observed may be attributed to the protein source and fermentation effects because the composition of formulations, in terms of ether extract and ash content, were within the recommended range for the nutritional needs of *M. rosenbergii* (S.T. & Belsare, 2021; D'Abramo & Sheen, 1993).

3.3 Amino Acid and Fatty Acid Profiles of Formulated Diets

The amino acid and fatty acid composition of raw materials and experimental diets are summarised in Table 4 and Table 5 respectively. As shown in Table 4, amino acid content increased significantly as a result of microbial hydrolysis process compared to SB, thus confirming the effectiveness of the microbial hydrolysis process. Specifically, substantial increases were observed in glutamic acid (7600.65 vs. 6971.10 mg/kg), aspartic acid (5217.41 vs. 4598.02 mg/kg), and leucine (3344.82 vs. 2850.18 mg/kg). The amino acid profile that the formulated diets (T1–T7) provide, details the amino acid available to the experimental prawns.

As per fatty acid analysis (Table 5), DBSF and MHBSF were found to be rich source of lauric acid (C12:0) with 4.51% and 4.00% of the total fatty acid composition, respectively. As a result, both the diets (T6 and T7) with higher inclusion of insects showed higher concentration of this medium-chain fatty acid at 0.40% and 0.77%, respectively. Even though the fish meal had been replaced, there were still essential polyunsaturated fatty acids present for all treatments. In particular, the percentage of eicosapentaenoic acid (C20:5n3) was kept at 0.07 % in T5, T6 and T7, while the percentage of docosahexaenoic acid (C22:6n3) was recorded at 0.01 % in T5 and T7. The total concentrations of Omega-3 ranged from 113.06 to 171.16 mg/100g in the experimental formulations to set the baseline of the fatty acid in the feeding trial.

3.4 Biomass Accumulation and Feed Utilization Efficiency

The growth performance and feed utilization efficiency of *M. rosenbergii* under experimental treatments are shown on Table 6. The initial weights of prawn post-larvae at the beginning of the trial ranged from 9.32 ± 1.23 g to 9.52 ± 0.82 g. At the end of the 60-day trial, the T6 group (50% MHBSF + MHSB + Bromelain) exhibited the highest growth performance in all the growth parameters, with the significantly highest final weight (18.80 ± 1.26 g), total weight gain (9.48 ± 0.95 g), and specific growth rate (SGR: 1.18 ± 0.17%/day ($p>0.05$). Survival rates of the formulated diets were also similar to those of other diets, ranging from 33.33 ± 0.00 to 40.00 ± 14.91 ($p>0.05$), showing that the survival rate of prawns was not affected by the formulated diets even when high amount of insects meal was used. In addition, T6 optimized feed economic efficiency with the least feed conversion ratio (2.24 ± 0.30). However, when fish meal was completely replaced by MHBSF (T7), the growth performance was significantly depressed compared to T6 (growth: 15.32 ± 1.86 g, SGR: 0.81 ± 0.14%/day, $p>0.05$).

3.5 Prawn Meat Proximate Composition and Exoskeleton Chitin Yield

The nutrient assimilation in the muscle tissue and deposition of chitin structure in the exoskeleton was significantly affected by dietary treatments (Table 6). In the proximate composition of prawn meat, T1 control had the highest percentage of crude protein which was 86.05 ± 0.03%, and the lowest percentage of intramuscular fat in T6 group was 6.48 ± 0.18% in comparison with the T1 group 4.21 ± 0.19% ($p<0.05$). This means that microorganisms' ability to release these highly bioavailable nutrients and fatty acids was efficiently utilized for energy storage. On the other hand, the yield of chitin from the prawn exoskeleton had exhibited a significant difference, with the highest chitin deposition in the T6 group (24.77 ± 2.15) which was significantly greater than that of the T1 control (12.78 ± 2.66) ($p<0.05$).

3.6 Hemolymph Biochemistry and Endogenous Enzymatic Shifts

There was a significant change in the internal enzymatic landscape and hemolymph metabolites that occurred when exogenous bromelain interacted with the microbially bioprocessed materials (Table 6). The average endogenous hepatopancreatic proteases activity in the T1 control group was 6.88 ± 0.60 mU/min/mg protein. In all the treatments, however, that were top-sprayed with bromelain (T2, T3, T4, and T6), the secretion was substantially reduced, ranging from 3.49 ± 0.73 to 3.89 ± 0.14 mU/min/mg protein ($p<0.05$). This indicates a feedback inhibition process which saves metabolic energy by providing external help in the form of proteolytic agents. At the same time, the lipase activity of T6 was found to be 47.33 ± 0.14 mU/ min/mg protein, a value that was the lowest.

Hemolymph metabolite profiles further elucidated digestive efficiency. Triglyceride levels significantly plummeted in T4 (9.41 ± 0.83 mg/dL) but increased sharply in groups fed microbially hydrolyzed diets, reaching 50.00 ± 3.00 mg/dL in T5, 48.24 ± 2.59 mg/dL in T6, and a peak of 73.53 ± 11.16 mg/dL in T7 ($p<0.05$). Furthermore, the endogenous amylase activity of T7 was found to have a dramatic increase (135.00 ± 3.79 mU/min/mg protein), along with significantly higher hemolymph glucose level (31.61 ± 1.44 mg/dL) and total blood protein (39.83 ± 1.25 mg/mL). These biochemical markers were able to demonstrate that the solid-state fermentation process was successful in breaking down restrictive feed matrices with resultant large amounts of released nutrients available to the systemic circulation.

Table 6: Somatic Growth Performance, Feed Utilization, Prawn Meat Proximate Composition, Hepatopancreatic Enzymes and Hemolymph Chemistry

Growth performance	Treatments						
	T1	T2	T3	T4	T5	T6	T7
Initial weight (g/prawn)	9.52 ± 0.82	9.47 ± 0.83	9.49 ± 1.15	9.43 ± 1.34	9.41 ± 1.10	9.32 ± 1.23	9.41 ± 1.07
Final weight (g/prawn)	15.02 ± 1.41 ^{a}	15.52 ± 2.30 ^{a}	15.56 ± 2.02 ^{a}	17.66 ± 1.98 ^{ab}	17.06 ± 1.83 ^{ab}	18.80 ± 1.26 ^{b}	15.32 ± 1.86 ^{a}
Weight Gain (g/prawn)	5.50 ± 0.72 ^{a}	6.05 ± 2.94 ^{ab}	6.07 ± 1.45 ^{ab}	8.23 ± 1.24 ^{bc}	7.65 ± 1.51 ^{abc}	9.48 ± 0.95 ^{c}	5.91 ± 1.32 ^{a}
ADG (g/prawn/day)	0.09 ± 0.01 ^{a}	0.10 ± 0.05 ^{a}	0.10 ± 0.02 ^{a}	0.14 ± 0.02 ^{b}	0.13 ± 0.02 ^{ab}	0.16 ± 0.02 ^{b}	0.10 ± 0.02 ^{a}
SGR (%/day)	0.76 ± 0.05 ^{a}	0.82 ± 0.37 ^{ab}	0.82 ± 0.16 ^{ab}	1.05 ± 0.16 ^{bc}	0.99 ± 0.19 ^{abc}	1.18 ± 0.17 ^{c}	0.81 ± 0.14 ^{ab}
Survival Rate (%)	33.33 ± 0.00	33.33 ± 0.00	40.00 ± 14.91	33.33 ± 0.00	33.33 ± 0.00	33.33 ± 0.00	33.33 ± 0.00
Feed intake (g/prawn/day)	0.36 ± 0.02	0.35 ± 0.05	0.36 ± 0.03	0.34 ± 0.02	0.35 ± 0.02	0.35 ± 0.03	0.37 ± 0.01
FCR	3.99 ± 0.56 ^{bc}	4.48 ± 2.55 ^{c}	3.77 ± 1.07 ^{abc}	2.54 ± 0.39 ^{ab}	2.83 ± 0.65 ^{abc}	2.24 ± 0.30 ^{a}	3.86 ± 0.85 ^{abc}
Prawn meat proximate composition and exoskeleton chitin yield (%)							
Moisture	8.46 ± 0.02 ^{c}	8.27 ± 0.02 ^{c}	7.50 ± 0.39 ^{a}	7.99 ± 0.02 ^{b}	8.32 ± 0.06 ^{c}	8.51 ± 0.02 ^{c}	8.53 ± 0.05 ^{c}
Crude Protein	86.05 ± 0.03 ^{f}	84.72 ± 0.16 ^{d}	84.90 ± 0.46 ^{d}	83.97 ± 0.48 ^{c}	85.53 ± 0.29 ^{e}	81.08 ± 0.06 ^{a}	83.07 ± 0.25 ^{b}
Ether Extract	4.21 ± 0.19 ^{a}	5.50 ± 0.20 ^{d}	5.16 ± 0.12 ^{c}	4.32 ± 0.07 ^{a}	5.08 ± 0.04 ^{c}	6.48 ± 0.18 ^{e}	4.60 ± 0.05 ^{b}
Crude Fiber	0.00 ± 0.00 ^{a}	0.00 ± 0.00 ^{a}	0.26 ± 0.04 ^{c}	0.00 ± 0.00 ^{a}	0.01 ± 0.01 ^{a}	0.20 ± 0.01 ^{b}	0.00 ± 0.00 ^{a}
Ash	5.18 ± 0.08 ^{b}	5.08 ± 0.08 ^{ab}	5.42 ± 0.04 ^{b}	4.71 ± 0.44 ^{a}	5.49 ± 0.11 ^{b}	5.46 ± 0.15 ^{b}	5.11 ± 0.28 ^{b}
Chitin	12.78 ± 2.66 ^{a}	23.39 ± 0.56 ^{c}	23.76 ± 2.98 ^{c}	17.21 ± 0.18 ^{b}	14.04 ± 1.37 ^{ab}	24.77 ± 2.15 ^{c}	14.12 ± 0.94 ^{ab}

Hepatopancreatic Enzymes and Hemolymph Chemistry							
Amylase (mU/min/mg protein)	100.87 ± 1.78 ^{d}	86.06 ± 0.39 ^{a}	99.45 ± 2.47 ^{cd}	84.60 ± 4.57 ^{a}	91.80 ± 3.28 ^{b}	94.42 ± 2.51 ^{bc}	135.00 ± 3.79 ^{e}
Lipase (mU/min/mg protein)	62.20 ± 0.42 ^{c}	69.19 ± 0.37 ^{ef}	69.92 ± 0.31 ^{f}	65.97 ± 1.68 ^{d}	53.33 ± 0.74 ^{b}	47.33 ± 0.14 ^{a}	67.88 ± 1.13 ^{e}
Protease (mU/min/mg protein)	6.88 ± 0.60 ^{c}	3.77 ± 0.81 ^{a}	3.62 ± 0.96 ^{a}	3.49 ± 0.73 ^{a}	4.45 ± 0.49 ^{ab}	3.89 ± 0.14 ^{a}	5.07 ± 0.38 ^{b}
Triglyceride (mg/dl)	26.62 ± 2.27 ^{b}	26.76 ± 3.13 ^{b}	26.91 ± 1.94 ^{b}	9.41 ± 0.83 ^{a}	50.00 ± 3.00 ^{c}	48.24 ± 2.59 ^{c}	73.53 ± 11.16 ^{d}
Glucose (mg/dl)	8.80 ± 0.59 ^{a}	13.29 ± 0.95 ^{b}	23.41 ± 1.37 ^{cd}	23.81 ± 1.42 ^{d}	28.24 ± 1.69 ^{e}	21.83 ± 0.70 ^{c}	31.61 ± 1.44 ^{f}

Note: Values within a given row designated by distinct superscripts differ significantly ($p < 0.05$)

3.7 Systemic Oxidative Stress and Lipid Peroxidation

The biomarkers of systemic oxidative stress and lipid peroxidation in *M. rosenbergii* showed significant differences between the different dietary treatments (Table 7 and Figure 1). A mean value of 1.47 ± 0.03 µmol/g protein was measured in the T1 control group, which served as the baseline amount of malondialdehyde. Lipid peroxidation was highest in T3 (50% DBSF) where the MDA level was significantly highest at 3.18 ± 0.37 µmol/g protein ($p<0.05$). This increase in MDA was accompanied by a significant increase in the activity of superoxide dismutase (136.97 ± 6.08 U/mg protein) and slight increase in the activity of catalase (109.33 ± 17.59 U/mg protein), which showed the presence of a higher compensative response to oxidative stress.

However, the combination (synergic) treatment in T6 (50% fermented replacement with bromelain) was able to effectively inhibit the oxidative damage with the lowest MDA level recorded in the experiment (1.41 ± 0.04 µmol/g protein). This decrease in lipid peroxidation was accompanied by significantly lowered SOD activity (24.62 ± 11.69 U/mg protein, $p<0.05$), which showed that the antioxidant status was more stable and less need for antioxidant enzyme mobilization. In this regard, however, the MDA levels and CAT activity returned to 2.06 ± 0.20 µmol/g protein and 83.28 ± 241.66 U/mg protein, respectively, in the 100% fermented replacement group (T7). The data indicates a significant variation in the activities of antioxidant enzymes and levels of lipid peroxidation markers, highlighting the importance of the inclusion level and processing condition of the defatted black soldier fly and soybean on the prawn's systemic oxidative status.

Table 7: Systemic Oxidative Stress Biomarkers in *M. rosenbergii*

Treatment	MDA (µmol/g protein)	SOD activity (U/mg protein)	CAT activity (U/mg protein)
T1	1.47 ± 0.03 ^{a}	122.67 ± 18.41 ^{cd}	277.88 ± 16.29
T2	1.62 ± 0.02 ^{a}	130.89 ± 6.91 ^{cd}	285.85 ± 90.60
T3	3.18± 0.37 ^{c}	136.97 ± 6.08 ^{d}	194.96 ± 115.27
T4	1.75 ± 0.17 ^{ab}	132.98 ± 9.30 ^{d}	177.56 ± 163.67
T5	1.45 ± 0.09 ^{a}	69.88 ± 8.80 ^{b}	188.74 ± 169.73
T6	1.41 ± 0.04 ^{a}	24.62 ± 11.69 ^{a}	168.92 ± 115.30
T7	2.06 ± 0.20 ^{b}	109.33 ± 17.59 ^{c}	83.28 ± 241.66

Note: Values within a given column designated by distinct superscripts differ significantly ($p < 0.05$)

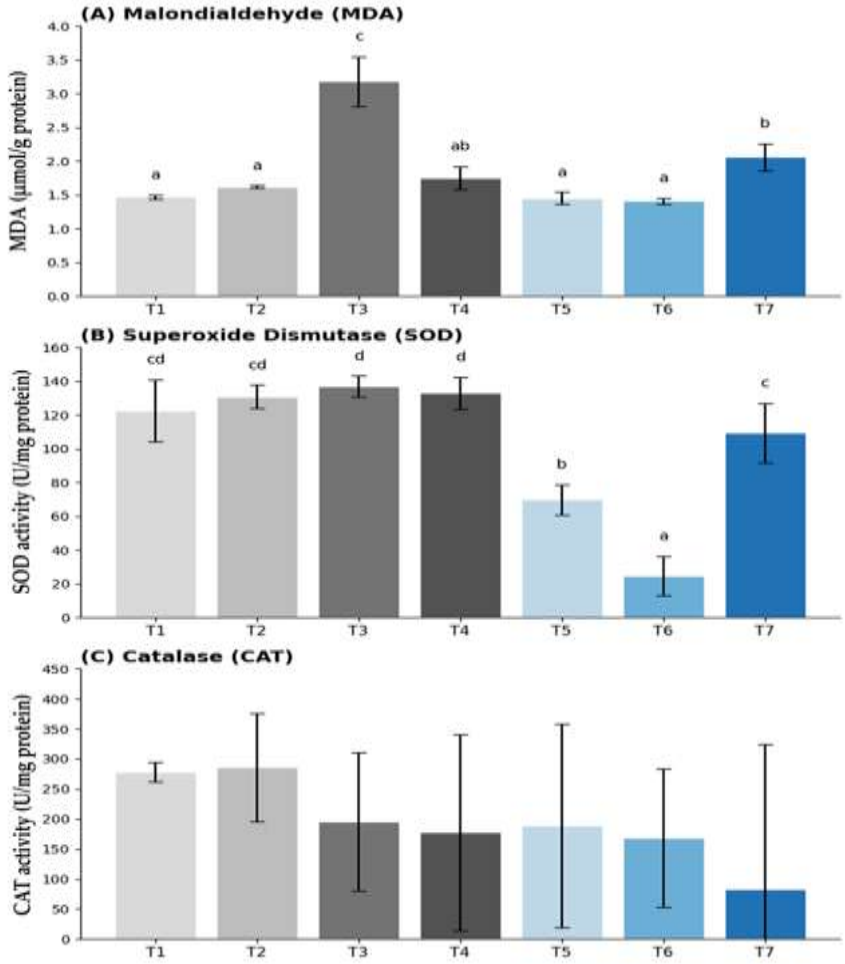

Figure 1 Systemic Oxidative Stress Biomarkers in *M. rosenbergii*. (a) Malondialdehyde, (b) Superoxide Dismutase, (c) Catalase

3.8 FTIR Spectral Analysis of Structural Chitin Disruption

Fourier-transform infrared Fourier-transform infrared spectroscopy was used to obtain a 'chemical signature' of the chitin extracted from the raw materials and the chitin extracted from prawn shells from the different dietary treatments (Figures 2). The comparative study showed that functional groups had experienced remarkable changes in the three main spectral regions, which suggested that the structure had been modified as a result of the microbial bioprocess and incorporation into the diet.

The spectra of DBSF showed sharp and narrow peaks in the hydrogen bonding region (3100–3400 cm-1) with peaks present in the O-H and N-H stretching vibration region of the spectrum, indicating a highly ordered crystalline chitin lattice with strong intermolecular and intramolecular hydrogen bonds. However, the MHBSF samples exhibited much greater broadening and decrease in peak intensity (Figure 3a), indicating disruption of this crystalline order. The chitin extracted from prawn shell showed the highest absorption (lowest transmittance) at 97.12% around 3253 cm-1 followed by T6 at 97.47% as depicted in figure 4a. These results suggest that the intermolecular hydrogen bonding network is dense, strong and highly ordered in the chitin structure of these groups. The T1 control, however, showed the lowest absorption (98.98% transmittance at 3239 cm^{-1}), indicating that the sample has the lowest crystallinity and the least orderly hydrogen bond arrangement.

Additional insights were gained from the Amide I (~1650cm^{-1}) C=O stretching) and Amide II (~1550cm^{-1}) N-H bending) bands, which were used to explore the integrity of the chitin-protein complex (Figure 3b). The DBSF spectra exhibited characteristic peaks, whereas the intensity of the peak and the spectral shift was significantly reduced in the MHBSF spectra. Among the prawn shell samples, T6 and T7 showed the most unique Amide I peak at the transmittance of 97.64% and 97.83% within the range of 1622-1628 cm-1. Similar to these results, T6 (1517 cm-1) and T7 (1558 cm^{-1}) also had the highest peak of the Amide II absorption band as depicted in Fig. 4b. This means that there is a protein-chitin complex that has a good number of peptides bound to the chitin in both groups T6 and T7. T1, on the other hand, exhibited virtually no protein protein absorption in this region (%T > 99.3%), suggesting that the proteinaceous components were either best removed or degraded in this group.

Last, for the glycosidic bond region (1030-1150 cm-1), associated with the chitin backbone's C-O-C asymmetric stretching, a clear decrease in peak intensity was found in MHBSF relative to DBSF. In the case of prawn shell chitin (Figure 3c), the most intense vibration was seen in the group T4 and T5 at 1030 cm-1 (%T ~96.5) indicating that the glycosidic bonds connecting the N-acetylglucosamine units were highly preserved. This indicates that T4 and T5 maintained the backbone of their primary structure more than other groups, and that it was less cleaved. As with the other areas, the T1 group demonstrated a reduction in resistance to structural cleavage with a transmittance of 98.88% at 1066 cm^{-1} as evidenced in Figure 4c, thus further indicating the dietary dependent changes in chitin molecular architecture.

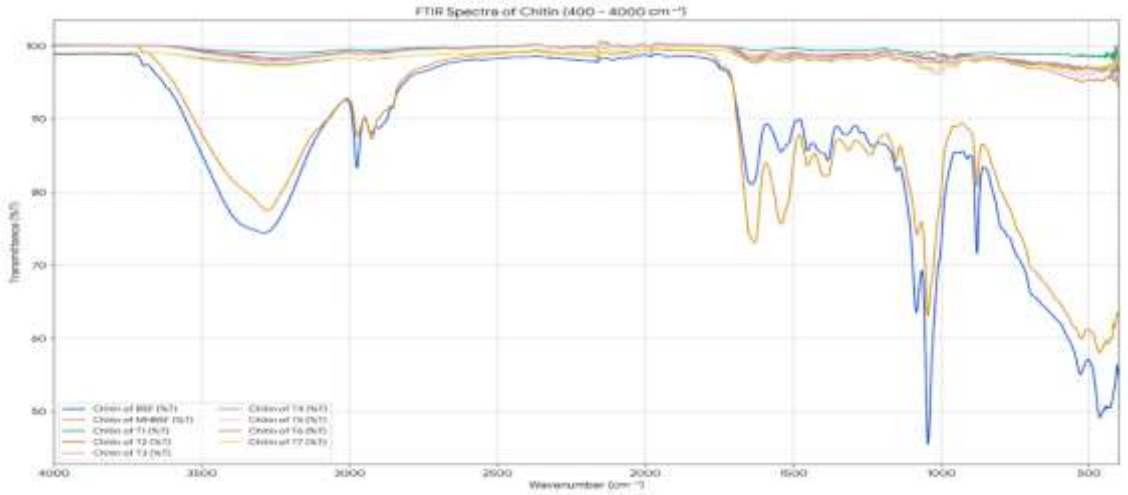

Figure 2 FTIR spectra of chitin extracted from giant freshwater prawn shells were analyzed across different dietary treatments and from black soldier fly (BSF)

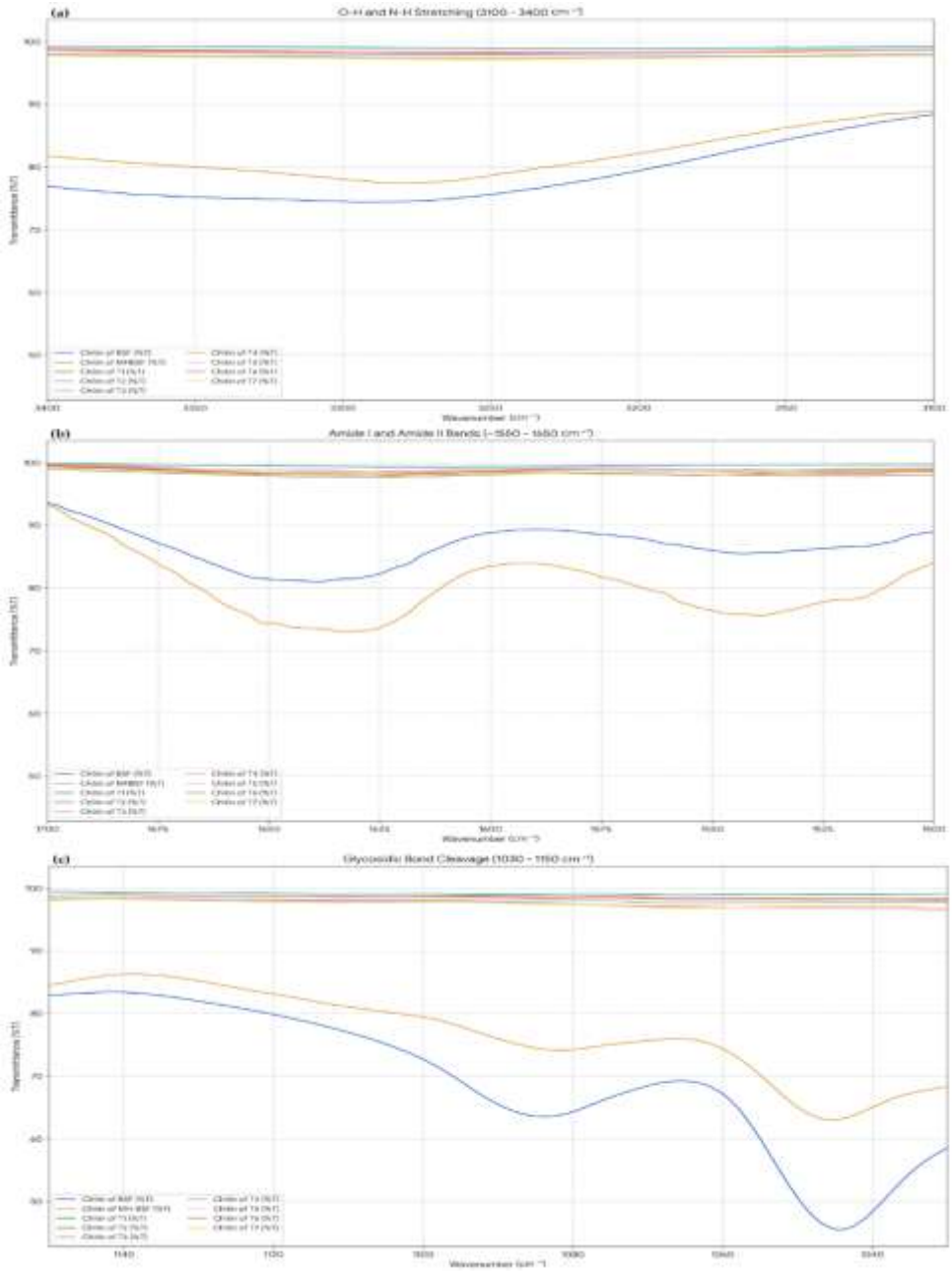

Figure 3 FTIR spectra of chitin extracted from DBSF and MHBSF: (a) Hydrogen Bonding Region (3100–3400 cm^{-1}), (b) Amide I and Amide II Bands (1550–1650 cm^{-1}), (c) Glycosidic Bond Region (1030–1150 cm^{-1})

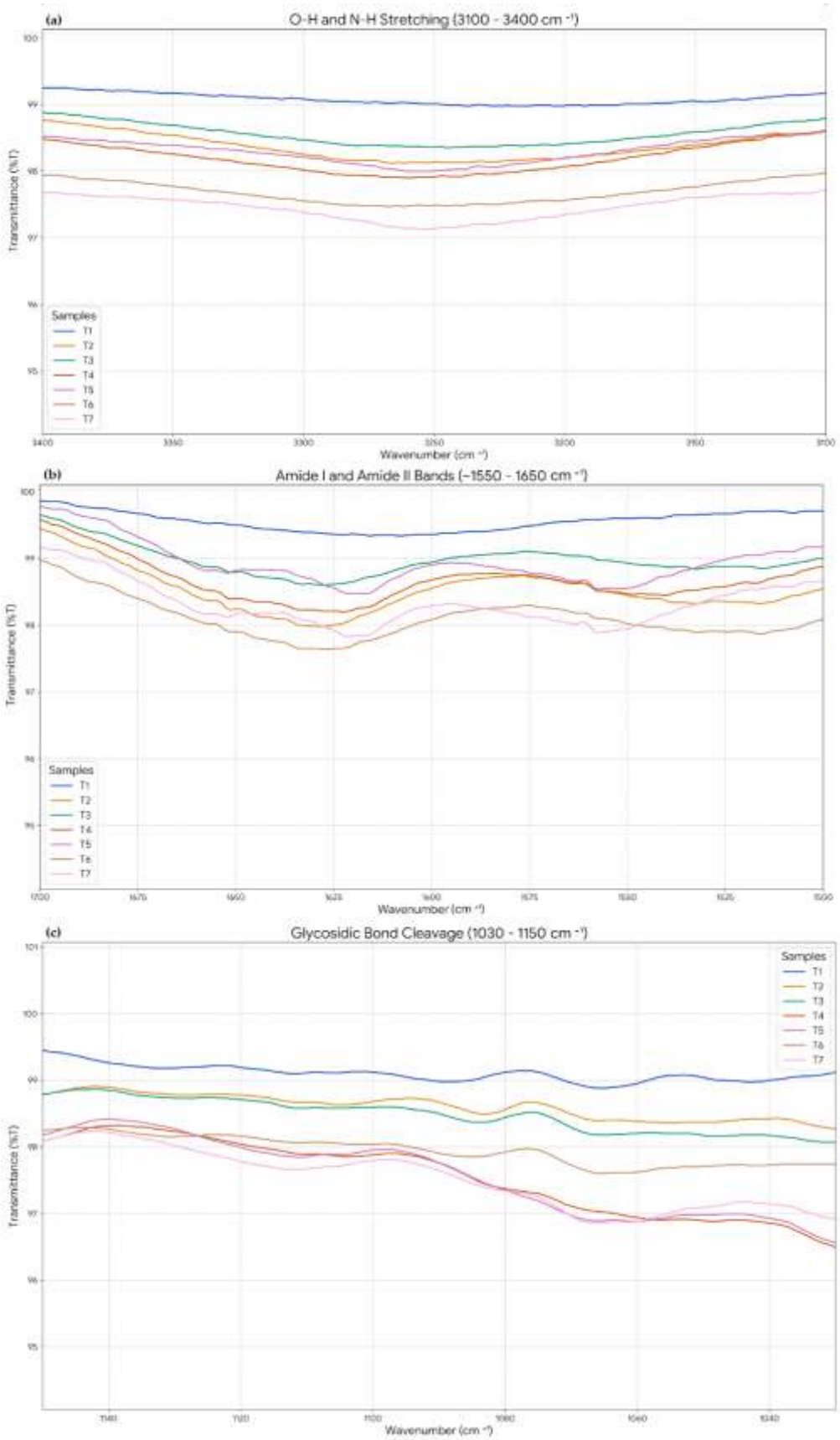

Figure 4 FTIR spectra of chitin extracted from giant freshwater prawn shells (T1-T7): (a) Hydrogen Bonding Region (3100–3400 cm^{-1}), (b) Amide I and Amide II Bands (1550–1650 cm^{-1}), (c) Glycosidic Bond Region (1030–1150 cm^{-1})

3.9 Scanning Electron Microscopy: Morphological Characteristics of Dietary Chitin and Prawn Cuticle

The surface of the DBSF and MHBSF was used to make high-resolution SEM micrographs to show a dramatic difference in surface topography between the two samples (Figure 5). The DBSF chitin had a dense, highly continuous and uniformly smooth surface with thick, block-like crystalline lamellae, which were tightly packed together. It was a strong, massive armour configuration with no obvious porosity or structural defects, and in its natural state was a physical barrier. The MHBSF exhibited significant structural disruptions and an extensive delamination, on the other hand. Previously intact chitin sheets were degraded and sponged into a highly porous

fractured micro-fibrillar matrix. Micrograph examination of the hydrolysed samples showed wide, cavernous fissures, irregular jagged edges and overlapping fragmented flakes. This transformation implies a great decrease in structure integrity and an exponential expansion of the activity surface of the matrix, caused by the microbial bioprocess.

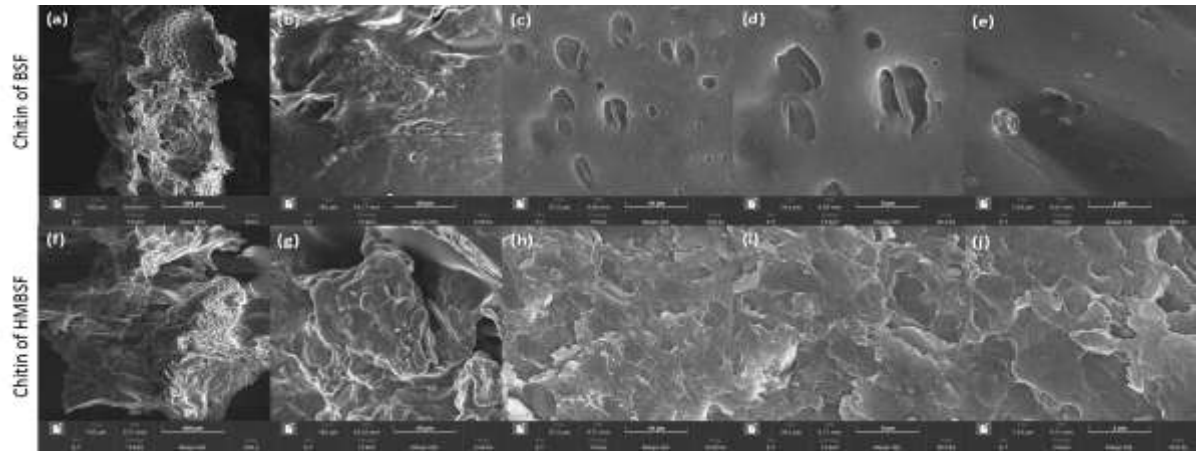

Figure 5 SEM images of chitin from DBSF and MHBSF: (a) BSF 200 µm, (b) BSF 50 µm, (c) BSF 10 µm, (d) BSF 5 µm, (e) BSF 2 µm, (f) MHBSF 200 µm, (g) MHBSF 50 µm, (h) MHBSF 10 µm, (i) MHBSF 5 µm, (j) MHBSF 2 µm

A detailed examination of the *M. rosenbergii* shells using SEM showed different structural changes in cuticular biomineralization when fed with different dietary treatments (Figure 6a–i). Control group topography (T1 and T2) showed typical smooth matrix with evenly distributed setal pits. On the other hand, the prawns fed raw insect meal (T3 and T4) showed signs of structural stress especially the 100% raw BSF group (T4) having irregular striations, scouring marks and ill-defined, elongated pitting. Under high magnification, it was noted that there was a break in continuity of the organic matrix, as the protective epicuticular layer was broken and the surface was brittle. But there was a significant improvement in shell morphology in prawns fed with the microbially hydrolyzed diets (T5, T6 and T7). The cuticle obtained from T6 (50 % MHBSF) was very smooth and clean and the pore structures were very clearly defined. The high magnification images of the T6 group showed that the nanofibrillar arrangement in the cuticle was very dense, suggesting a highly organized and robust biomineralization process.

3.10 Intestinal Histomorphology and Mucosal Health

The cross-section SEM analysis of the intestinal tracts of *M. rosenbergii* showed a remarkable difference between raw and hydrolyzed dietary treatments (Fig. 6j–u). The intestinal mucosa in the raw BSF group (T3 and T4) showed physical damage to the mucosa, the mucosal folds were blunted, shortened and greatly flattened, and secondary branching, necessary for optimum nutrient uptake, was lacking. This architectural failure was accompanied by a greater than usual increase of the luminal space and a thinned, inextensible intestinal wall (Figure 6j–k). In contrast, 50% and 100% MHBSF (T6 and T7) resulted in histological hyperproliferation. The mucosal folds in these groups were very complex and deep with a dense, fractal-like branching which protruded dramatically into the lumen (Figure 6m – n and t – u). This dense mucosal structure almost obliterated the intestinal lumen, which allowed the feed to come into close contact with the mucosa to a maximum extent. Mucosal health and absorptive ability was superior with the microtopography remaining pristine across these hydrolysed treatments, without any sign of necrotic sloughing or abrasive damage.

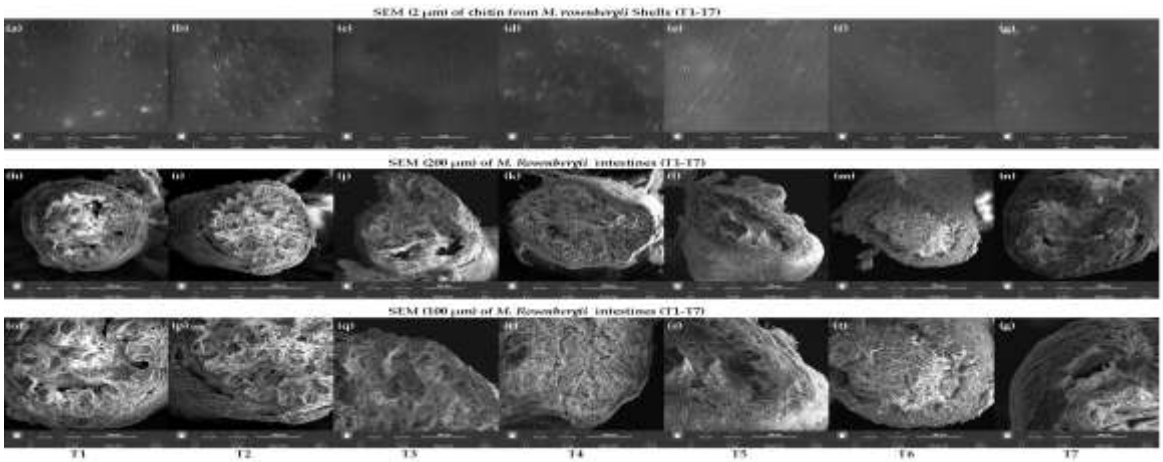

Figure 6 SEM image of chitin from *M. rosenbergii shells T1-T7* (2 µm, a-g) *and intestines T1-T7* (200 µm; h-m and 100 µm; o-u)

4. Discussion

This current multi-disciplinary study unravels the complex biological and biochemical interactions that take place when defatted black soldier fly and soybean meal are used in the diet of *M. rosenbergii*. The in vitro nutritional value of these proteins is encouraging, but their use has been restricted due to their physical and anti-nutritional properties, including the indigestibility of proteins and lipids, and the sequestration of essential nutrients by the rigid crystalline matrix of insect chitin (Nairuti et al., 2021),(Eggink et al., 2022). This recalcitrant chitin structure is not degraded by many aquatic species as there is no endogenous chitinase activity, which has been shown to have a negative effect on feed intake, growth performance and nutrient digestibility of various aquaculture species (General et al., 2023). But, the enzymatic pre-treatment, such as microbial hydrolysis or supplementation of bromelain can break this barrier leading to enhanced nutrient bioavailability and reduced anti-nutritional effects (Wang et al., 2024). Our findings clearly showed that the combination of the microbial solid-state fermentation (co-inoculation of R. microsporus and L. reuteri) and exogenous supplementation of bromelain could be the key to overcome these physiological limitations and improve nutrient bioavailability and intestinal health (Chen et al., 2025). This method not only enhances the general palatability and assimilation of alternate protein sources such as larvae meal of BSF but also has a positive effect on the growth rate and feed conversion ratio of *M. rosenbergii* (Riolo et al., 2023).

4.1 Nutritional Synergy, "Energy Sparing," and the "Sweet Spot" (The T6 Paradigm)

The main finding of this investigation is that the biological optimum for *M. rosenbergii* is T6 (50% replacement with microbially hydrolyzed BSF and soybean meal with bromelain). The final weight (18·80 ± 1·26 g), Specific Growth Rate (1·18 ± 0·17 %/day) and Feed Conversion Ratio (2·24 ± 0·30) were all the best in this group. This optimal performance is not simply from nutrient provision but ultimately is the consequence of a multi-layered physiological synergy that fundamentally changes the metabolic energy allocation of the prawn.

Endogenous protease secretion also is significantly reduced in T6 (from 6.88 ± 0.60 to 3.89 ± 0.14 mU/min/mg protein), which is another indication of the strong 'energy-sparing' effect. In the traditional way, prawns invest a lot of metabolic effort in the production and release of digestive enzymes for the degradation of complex proteins (Mantoan et al., 2021). This decrease in metabolic overhead freed more energy to be devoted to muscle protein synthesis which in turn correlated directly with the maximum SGR (1.18 ± 0.17 %/day) recorded for this group.

4.1.1 Microbial Demolition and the Porous Chyme Matrix

This synergy depends on biochemical enrichment and physical demolition of the feed matrix before it is ingested; the raw α-chitin serves as an extremely restrictive, crystalline "cage" that encases and sequesters digestible proteins and lipids within the recalcitrant matrix, which protects them from being accessible to the prawn's endogenous enzymes (Eggink et al., 2022).

At the same time, the fermentation process can neutralize the anti-nutritional factors of soybean meal, and the heat-stable factors such as trypsin inhibitors, lectin and phytic acid in soybean meal can also be neutralized, and the short-chain peptide content of the neutralized meal can also be enriched, effectively filling the nutrition gap caused by 50% reduction in the amount of marine fish meal(Zhang et al., 2021).

4.1.2 Exogenous Bromelain and the "Energy Sparing" Hypothesis

The optimized chyme then passes into the digestive system and a second synergy comes into play with the addition of bromelain, an exogenous broad-spectrum thiol endopeptidase. Bromelain breaks down dietary proteins to smaller peptides (Klahan et al., 2023). Important, the biochemical burden of proteolysis is taken up by the exogenous bromelain, and the prawn's physiology starts a significant feedback inhibition. This is reflected in the substantial decrease in the endogenous protease activity in Group T6 (3.89 ± 0.14 mU/min/mg protein) compared with T1 (control) (6.88 ± 0.60 mU/min/mg protein). This suppression is a very favourable ‘energy-sparing’ effect. Moreover, the close relationship between the physiological balance and the growth of T6 is reinforced by its excellent antioxidant status. The remarkable decrease of malondialdehyde level to 1.41 ± 0.04 μmol/g protein, the lowest level among the malondialdehyde levels found in this trial, suggests that combination of microbially hydrolyzed nutrients and bromelain seemed to be a powerful "metabolic buffer". The T6 diet reduced the generation of reactive oxygen species through the disruption of the structural barrier by fermentation (Xie et al., 2021), while bromelain allows the proteins to be absorbed easily.

This decrease of oxidative stress directly coincides with improvement in biomass accumulation. In aquatic species, a high metabolic cost is usually linked to cellular repair, detoxification and enhancement of antioxidant defenses to fight against lipid peroxidation (Fadhlaoui & Couture, 2016). The T6 group was able to redirect energy that would normally be used in homeostasis or repairing tissue into muscle growth and the synthesis of exoskeleton due to this oxidative crisis and the attainment of “metabolic tranquility” (Wiszniewski et al., 2019). This reallocation of the energy budget primarily accounts for the maximum value for specific growth rate ($1.18 \pm 0.17%$/day) and higher survival. Therefore, bromelain acts as a digestive aid and the first mentioned source indicates that it could also be an immunomodulator in other shrimp species (Klahan et al., 2023).

4.1.3 MCFA Utilization and Intestinal Hyperplasia

Furthermore, there were significant amounts of lauric acid (C12:0), a functional medium-chain fatty acid, introduced with the inclusion of MHBSF. The MCFAs do not form complex micelle, and are directly carried towards the hepatopancreas where they are rapidly subjected to β-oxidation. This is an efficient systemic ATP supply for somatic growth (Yang et al., 2025).

Morphologically, the prawn adapted to this nutrient-rich environment as indicated by the adaptive intestinal hyperplasia, which was observed with SEM micrographs of T6 showing massively proliferated and complex mucosal folds, exponentially increasing the absorptive surface area (Chen et al., 2025). Such hyper-proliferated architecture guarantees quick absorption of a large number of short-chain peptides, MCFAs, and consequently, optimal intramuscular lipid deposition and explosive somatic growth are observed in the T6 group. This combination of an available nutrient matrix and improved mucosal structure helps to make the gut a very efficient absorption unit, with reduced metabolic strain.

4.2 Metabolic Overload and Antioxidant System Collapse at 100% Replacement (T7)

Although the dietary approach for T6 was physiologically successful, the metabolic threshold of 100% fermented insect meal to substitute the fishmeal was observed in Group T7. Although the MHBSF is highly digestible, growth performance in T7 did not improve but returned to baseline values (T1 control) (Chen et al., 2021) because of the combination of rapid nutrient absorption, environmental instability, and the subsequent breakdown of the hepatic antioxidant system (Guerreiro et al., 2022; Louzã et al., 2024; Sharifinia et al., 2023).

Systemic hyperlipidemia was seen in T7 (73.53 ± 11.16 mg/dL triglycerides) indicating a threshold of 'nutrient flooding' (that is, protein to energy ratio in feed is higher than the physiological ability of the organism to process them). Microbial hydrolysis played a significant role in increasing the availability of nutrients and the 100% replacement strategy may have caused a too high influx of lipids and amino acids which rapidly resulted in ‘hepatopancreas exhaustion'. The hepatic failure observed and the simultaneous increase of oxidative stress markers further emphasizes this metabolic bottleneck. These results suggest that pre-digestion via fermentation is very beneficial, but that a very precise level of replacement is needed to prevent an overload of the prawns' homeostasis/detoxification processes.

4.2.1 Nutrient Flooding, Hyperlipidemia, and Glycemic Stress

The complete substitution of fish meal by 100% MHBSF caused the feed pellet to fragment and the prawn's metabolic balance. The highly hydrolysed and water soluble peptides and lipids were released into gastrointestinal tract at an overwhelming velocity (Irungu et al., 2018), termed as “Massive Nutrient Flooding”, due to the absence of binding properties inherent in marine proteins. This resulted in a state of systemic hyperlipidaemia with the hemolymph triglycerides level being 73.53 ± 11.16mg/dl. At the same time, there was a significant stress response of the physiological system, which was reflected by the increase in endogenous amylase to 135.00 ± 3.79 mU/min/mg protein and blood glucose to 31.61 ± 1.44 mg/dL (Susilo & Rachmawati, 2020). These glycemic markers are a sign of gluconeogenesis due to stress and metabolic fatigue (Chen et al., 2021). Also, excessive feeding of dietary chitin derivatives, without supplementing with conventional proteins, can cause metabolic adjustments that focus on detoxification rather than growth.

4.2.2 Environmental Leaching, Oxidative Damage, and Antioxidant Exhaustion

Simultaneously, the very exposed lipid fractions of the 100% MHBSF diet were very sensitive to rapid autoxidation, producing toxic lipid peroxidation products like malondialdehyde precursors, which entered the system before they were consumed (Secci et al., 2018; Vieira et al., 2017).

The combined hepatopancreatic hyperlipidaemia and the oxidized lipids consumed resulted in excess production of reactive oxygen species, which led to overloading of hepatopancreatic defense mechanisms (Wang et al., 2021). Oxidative stress indicators showed that malondialdehyde (MDA) levels significantly increased (2.06 ± 0.20 μmol/g protein) and that the activity of catalase (CAT) significantly decreased (83.28 ± 24.16 U/mg protein), in a catastrophic manner, in the metabolic failure of T7.

The very large standard deviation of the CAT activity of Group T7 (83.28 ± 241.66 U/mg protein) is a good indicator of the various physiological reactions to extreme metabolic stress. This statistical variance indicates that at 100% replacement level the prawns reached a 'physiological tipping point', a 'tipping point' in their individual adaptive capacities, that varied in speed.

4.3 Mechanical Abrasion and Synergistic Inflammation: The Perils of Raw Ingredients (T3 and T4)

The present investigation has clearly shown the serious physiological effects of the unfermented, raw insect (T3) and plant (T4) meals in the crustacean feed. The internal micro-anatomy of prawns fed raw BSF diet (T4) was in severe physiological crisis despite the addition of exogenous bromelain which was sufficient to allow the prawns to obtain nutrients and survive moderately (Chen et al., 2021).

4.3.1 Physical Trauma Induced by α-Chitin

The key problem with this crisis is the abrasive and crystalline nature of raw α-chitin which is found in unfermented BSF exoskeletons. SEM analysis of the intestine showed unfermented chitinous shards in the digesta mass, which was very dense and impacted in the intestinal lumen. The width of the delicate intestinal mucosal folds decreased, as was the height of the intestinal mucosal folds, and the structure of the intestinal epithelial cells was damaged to the intestinal epithelial cell structure (Chen et al., 2021). This trauma is known to drastically reduce the functional absorptive surface area and thus directly contribute to the poor utilization of nutrients and higher FCR observed in the raw ingredient treatments (Henry et al., 2015). Black Soldier Fly meal is known to cause gastrointestinal lining damage and blockage of growth without any modifications to the structure (Chen et al., 2021).

4.3.2 The Oxidative Crisis and Cellular Peroxidation

This mechanical injury combined with the effect of chemical irritation caused by unfermented soybean anti-nutritional factors elicited a systemic inflammatory response, and oxidative stress parameters indicated that continuous cellular damage during this process created a large amount of free radical (Peng et al., 2023). The level of malondialdehyde in group T3 (50% raw BSF + raw SB) was significantly increased to 3.18 ± 0.37 μmol/g protein which was the highest in the trial, and the activity of superoxide dismutase was increased significantly to 136.97 ± 6.08 U/mg protein as the hepatopancreas tried to counteract the superoxide radicals. High MDA levels combined with the high antioxidant enzyme activities indicate that ROS might have overwhelmed the protection of cells, resulting in lipid peroxidation of hepatopancreatic membrane (Duan et al., 2018). On the other hand, the microbial solid-state fermentation is a crucial prerequisite in biotechnology for gastrointestinal welfare; the optimal fermented diet (T6) has eliminated the abrasive threat and generated antioxidant peptides, thus solving the oxidative crisis in raw treatments, with the lowest MDA levels (1.41 ± 0.04 μmol/g protein) and minimal SOD activation (24.62 ± 11.69 U/mg protein).

4.4 Shell Rejuvenation, Biomineralization, and Dual-Action Functional Feeds

The fermented diet was synergized and apart from enhancing the internal health of hepatopancreas and intestine, probably contributed towards the integrity of the prawn's exoskeleton and its immunological resilience (Kulkarni et al., 2020). The SEM image of the exoskeleton showed the prawns fed fermented diets (T5 and T6) were producing very smooth, clean, and well-formed exoskeleton with no signs of microfissures and stress fractures as seen in the prawns fed raw insect meal (T3 and T4).

The functional integrity of the diet is maintained even though the pellets are produced by a high temperature extrusion process (up to 140°C) by means of a robust dual-action mechanism. COS produced during fermentation are high thermally stable prebiotics (Kim et al., 2024) as the first. Thermal processing of COS, even at temperatures exceeding 200°C, does not affect the structural integrity of the glycosidic bonds, which are key for selectively promoting growth of beneficial bacteria, including Lactobacillus spp., as evidenced in academic studies (Kim et al., 2024; Castillo et al., 2017). These COS selectively stimulate growth of beneficial bacteria that in turn facilitates better absorption of essential nutrients and competitively inhibits opportunistic pathogens from the aquatic environment(Tayyab et al., 2025) and improve antioxidant activity(Guan et al., 2019).

Second, heat-inactivated biomass of *Rhizopus microsporus* and its stable fermentation metabolites act as postbiotics(Ismail & Emran, 2020). These non-viable microbial components offer essential immunomodulatory advantages, aiding in improved overall health despite being heat-killed during feed processing (Da et al., 2024). These highly bioavailable COS oligomers and postbiotic fractions are much easier to uptake by the intestinal epithelium into the hemolymph than intact chitin because of the low molecular weight. In this way the prawn can easily re-use these "pre-fabricated" chitin building blocks in the biomineralization of the cuticule at the epidermis. This gives a cheap and easy source of structural precursors (metabolically) and allows for rapid and perfect exoskeleton synthesis (Gonçalves, 2021).

Biomineralization of *M. rosenbergii* is essential for the smooth molting cycle and for minimizing molting mortality (Khasani et al., 2012). In addition, the healthy cuticle is the main physical barrier against environmental pathogens, making them more likely to survive and to produce a higher quality crop (Kulkarni et al., 2020). Microbial fermentation creates a prebiotic and postbiotic matrix from a structural barrier that is bioavailable to the prawn's entire physiological interface, ranging from gut lumen to the external exoskeleton (Sha et al., 2024).

5. Conclusion

The present multi-tiered investigation clearly shows that co-innoculation of *Rhizopus microsporus* and *Lactobacillus reuteri* along with the exogenous supplementation of bromelain is an effective biotechnological approach to production of alternative aquafeeds for *Macrobrachium rosenbergii.* Biological optimum biological optimum (T6) was found to be 50% fish meal replacement with better growth performance (Final Weight: 18.80 ± 1.26 g, FCR: 2.24 ± 0.30) and maximum specific growth rate (1.18 ± 0.17%/day) supported by empirical data. The T6 paradigm relies on two synergic factors that contribute to the success: the microbial pre-digestion that transforms the rigid matrix of the α-chitin to a porous, bioaccessible chyme and the supplementation of bromelain which allows rapid proteolysis and produces a tremendous "energy-sparing" effect by down-regulating the endogenous secretion of protease. These mechanisms all contributed to the reduction of systemic oxidative stress as reflected in the lowest MDA level recorded (1.41 ± 0.04μmol/g protein), and the promotion of intestinal health by hyper-proliferation of mucosal absorptive surfaces. In addition, this optimal diet also allowed optimal exoskeleton synthesis, with the highest chitin content (24.77 ± 2.15%) and with the cleanest cuticular morphology. In contrast, a higher level of replacement (100% – T7) caused hyperlipidaemia (triglycerides >73 mg/dL), glycemic stress and a loss of antioxidant capacity, which was termed "metabolic overload. This highlights the 50% replacement approach as a scientifically proven pathway to minimize fish meal use while maximizing the physiological well-being, gut health, and harvest of decapod crustaceans in sustainable aquaculture practices.

References

1. Arbon, P., Martinez, M. A., Jerry, D. R., & Condon, K. (2023). Towards a ‘systems’ approach for viral challenge experiments in shrimp: Reporting guidelines for publication. *Reviews in Aquaculture*, *16*(2), 923. https://doi.org/10.1111/raq.12877
2. Barrera-León, M., Terán-Cabanillas, E., Avena-Bustillos, R. J., Cárdenas-Torres, F. I., Amézquita-López, B. A., Gómez-Favela, M. A., Alemán-Hidalgo, D. M., & Arias-Gastélum, M. (2025). Transformation of Brewer’s Spent

Grain Through Solid-State Fermentation: Implications for Nutrition and Health. *Recycling*, *10*(5), 170. https://doi.org/10.3390/recycling10050170
3. Bezerra, R. de S., Lins, E. J. F., Alencar, R. B., Paiva, P. M. G., Chaves, M. E. C., Coelho, L. C. B. B., & Carvalho, L. B. de. (2005). Alkaline proteinase from intestine of Nile tilapia (Oreochromis niloticus). *Process Biochemistry*, *40*(5), 1829. https://doi.org/10.1016/j.procbio.2004.06.066
4. Blasco, J., Vélez, E. J., Perelló-Amorós, M., Azizi, S., Capilla, E., Fernández-Borràs, J., & Gutiérrez, J. (2021). Recombinant Bovine Growth Hormone-Induced Metabolic Remodelling Enhances Growth of Gilthead Sea-Bream (Sparus aurata): Insights from Stable Isotopes Composition and Proteomics. *International Journal of Molecular Sciences*, *22*(23), 13107. https://doi.org/10.3390/ijms222313107
5. Brigode, C., Hobbi, P., Jafari, H., Verwilghen, F., Baeten, E., & Shavandi, A. (2020). Isolation and physicochemical properties of chitin polymer from insect farm side stream as a new source of renewable biopolymer. *Journal of Cleaner Production*, *275*, 122924. https://doi.org/10.1016/j.jclepro.2020.122924
6. Castillo, L. A., Farenzena, S., Pintos, E., Rodríguez, M. S., Villar, M. A., García, M. A., & López, O. V. (2017). Active films based on thermoplastic corn starch and chitosan oligomer for food packaging applications. *Food Packaging and Shelf Life*, *14*, 128. https://doi.org/10.1016/j.fpsl.2017.10.004
7. Chen, S., Maulu, S., Wang, J., Xie, X., Liang, X., Wang, H., Wang, J., & Xue, M. (2023). The application of protease in aquaculture: Prospects for enhancing the aquafeed industry. *Animal Nutrition*, *16*, 105. https://doi.org/10.1016/j.aninu.2023.11.001
8. Chen, Y., Chi, S., Zhang, S., Dong, X., Yang, Q., Liu, H., Tan, B., & Xie, S. (2021a). Evaluation of the Dietary Black Soldier Fly Larvae Meal (Hermetia illucens) on Growth Performance, Intestinal Health, and Disease Resistance to Vibrio parahaemolyticus of the Pacific White Shrimp (Litopenaeus vannamei). *Frontiers in Marine Science*, *8*. https://doi.org/10.3389/fmars.2021.706463
9. Chen, Y., Chi, S., Zhang, S., Dong, X., Yang, Q., Liu, H., Tan, B., & Xie, S. (2021b). Effect of black soldier fly (Hermetia illucens) larvae meal on lipid and glucose metabolism of Pacific white shrimp Litopenaeus vannamei. *British Journal Of Nutrition*, *128*(9), 1674. https://doi.org/10.1017/s0007114521004670
10. Chen, Z.-Y., Li, Q., Sheng, R., Zhang, J., Guo, J., Tan, P., Bao, S., Liu, Y., Kong, Y., Bai, H., & Ding, Z. (2025). *Effects of defatted black soldier fly larvae meal on growth, nutrient digestibility, hepatopancreas biochemistry, intestinal microbiota, and phosphorus discharge of giant freshwater prawn (Macrobrachium rosenbergii)*. https://doi.org/10.1016/j.aninu.2025.08.001
11. Da, M., Sun, J., Ma, C., Li, D., Li, D., Wang, L., & Chen, F. (2024). Postbiotics: Enhancing human health with a novel concept. *eFood*, *5*(5). https://doi.org/10.1002/efd2.180
12. D'Abramo, L. R., & Sheen, S. (1993). Polyunsaturated fatty acid nutrition in juvenile freshwater prawn Macrobrachium rosenbergii. *Aquaculture*, *115*, 63. https://doi.org/10.1016/0044-8486(93)90359-7
13. Duan, Y., Zhang, J., Wang, Y., Liu, Q., & Xiong, D. (2018). Nitrite stress disrupts the structural integrity and induces oxidative stress response in the intestines of Pacific white shrimp Litopenaeus vannamei. *Journal of Experimental Zoology Part A Ecological and Integrative Physiology*, *329*(1), 43. https://doi.org/10.1002/jez.2162
14. Eggink, K. M., Pedersen, P. B., Lund, I., & Dalsgaard, A. J. T. (2022). Chitin digestibility and intestinal exochitinase activity in Nile tilapia and rainbow trout fed different black soldier fly larvae meal size fractions. *Aquaculture Research*, *53*(16), 5536. https://doi.org/10.1111/are.16035
15. Fadhlaoui, M., & Couture, P. (2016). Combined effects of temperature and metal exposure on the fatty acid composition of cell membranes, antioxidant enzyme activities and lipid peroxidation in yellow perch (Perca flavescens). *Aquatic Toxicology*, *180*, 45. https://doi.org/10.1016/j.aquatox.2016.09.005
16. General, B. M., Julius, O. M., James, M., & Rono, K. (2023). Growth performance and carcass composition of African catfish (Clarias gariepinus Burchell, 1822) fed on black soldier fly (Hermetia illucens Linnaeus, 1758) larvae based diets. *African Journal of Agricultural Research*, *19*(3), 216. https://doi.org/10.5897/ajar2022.16235
17. Giménez, M. I., Studdert, C. A., Sánchez, J. J., & De Castro, R. E. (2000). *Extracellular protease of Natrialba magadii: purification and biochemical characterization*.
18. Gonçalves, R. (2021). Ontogenetic Development and Nutritional Requirements in Early Life Stages of the European Lobster (Homarus gammarus, L.). *Research Portal Denmark*, 170. https://local.forskningsportal.dk/local/dki-cgi/ws/cris-link?src=dtu&id=dtu-cc0bee56-1810-4380-8e78-a0f0250446de&ti=Ontogenetic%20Development%20and%20Nutritional%20Requirements%20in%20Early%20Life%20Stages%20of%20the%20European%20Lobster%20(%3Ci%3EHomarus%20gammarus%3C%2Fi%3E%2C%20L.)
19. Guan, G., Azad, Md. A. K., Lin, Y., Kim, S. W., Tian, Y., Liu, G., & Wang, H. (2019). Biological Effects and Applications of Chitosan and Chito-Oligosaccharides. *Frontiers in Physiology*, *10*, 516. https://doi.org/10.3389/fphys.2019.00516
20. Gutiérrez-Pérez, E. D., Vázquez-Juárez, R., Magallón-Barajas, F. J., Martínez, M. Á., Escobar-Zepeda, A., & Magallón-Servín, P. (2022). How a holobiome perspective could promote intensification, biosecurity and eco-efficiency in the shrimp aquaculture industry. *Frontiers in Marine Science*, *9*. https://doi.org/10.3389/fmars.2022.975042
21. Hashim, S. O., Delgado, O. D., Martínez, M. A., Kaul, R.-H., Mulaa, F., & Mattiasson, B. (2005). Alkaline active maltohexaose-forming α-amylase from Bacillus halodurans LBK 34. *Enzyme and Microbial Technology*, *36*(1), 139. https://doi.org/10.1016/j.enzmictec.2004.07.017
22. Henry, M., Gasco, L., Piccolo, G., & Fountoulaki, E. (2015). Review on the use of insects in the diet of farmed fish: Past and future. *Animal Feed Science and Technology*, *203*, 1. https://doi.org/10.1016/j.anifeedsci.2015.03.001

23. Hittinahalli, C. M., Mal, B. C., Reddy, A. K., Verma, A. K., & Pattusamy, A. (2023). Design and performance evaluation of rotating biological contactors for recirculating freshwater prawn (Macrobrachium rosenbergii) hatchery using artificial seawater. *Aquaculture International*, *31*(4), 1837. https://doi.org/10.1007/s10499-023-01060-4
24. Irungu, F. G., Mutungi, C., Faraj, A. K., Affognon, H., Kibet, N., Tanga, C. M., Ekesi, S., Nakimbugwe, D., & Fiaboe, K. K. M. (2018). Physico-chemical properties of extruded aquafeed pellets containing black soldier fly (Hermetia illucens) larvae and adult cricket (Acheta domesticus) meals. *Journal of Insects as Food and Feed*, *4*(1), 19. https://doi.org/10.3920/jiff2017.0008
25. Ismail, S. A., & Emran, M. A. (2020). Direct microbial production of prebiotic and antioxidant chitin-oligosaccharides from shrimp byproducts. *Egyptian Journal of Aquatic Biology and Fisheries*, *24*(4), 181. https://doi.org/10.21608/ejabf.2020.98021
26. Kalaiselvan, P., Devi, N. C., Deepti, M., Devi, A. A., Akamad, K., Dheeran, P., Debbarma, S., Vadivel, D., & Vekariya, R. D. (2025). Solid-state fermentation—a sustainable future technology in aquafeeds? *Frontiers in Marine Science*, *12*. https://doi.org/10.3389/fmars.2025.1669719
27. Ketnawa, S., Chaiwut, P., & Rawdkuen, S. (2012). Pineapple wastes: A potential source for bromelain extraction. *Food and Bioproducts Processing*, *90*(3), 385. https://doi.org/10.1016/j.fbp.2011.12.006
28. Khasani, I., Ridzwan, N. S., & Jones, C. (2012). EFFECT OF CALCIUM SUPPLEMENTATION ON GIANT FRESHWATER PRAWN (Macrobrachium rosenbergii) MOULTING AND EGG QUALITY. *Indonesian Aquaculture Journal*, *7*(1), 29. https://doi.org/10.15578/iaj.7.1.2012.29-36
29. Kim, H., Cheon, G. Y., Kim, J. H., Choi, R., Kim, I.-W., Suh, H. J., Hong, K., & Han, S. (2024). Preparation of chitosan oligosaccharides from chitosan of tenebrio molitor and its prebiotic activity. *Applied Biological Chemistry*, *67*(1). https://doi.org/10.1186/s13765-024-00937-z
30. Klahan, R., Deevong, P., Wiboonsirikul, J., & Yuangsoi, B. (2023). Growth Performance, Feed Utilisation, Endogenous Digestive Enzymes, Intestinal Morphology, and Antimicrobial Effect of Pacific White Shrimp (Litopenaeus vannamei) Fed with Feed Supplemented with Pineapple Waste Crude Extract as a Functional Feed Additive. *Aquaculture Nutrition*, *2023*, 1. https://doi.org/10.1155/2023/1160015
31. Kulkarni, A., Sreedharan, K., Anand, D., Uthaman, S. K., Otta, S. K., Karunasagar, I., & Rajendran, K. V. (2020). *Immune responses and immunoprotection in crustaceans with special reference to shrimp*. https://doi.org/10.1111/raq.12482
32. Mantoan, P. V. L., Ballester, E. L. C., Ramaglia, A. C., & Augusto, A. (2021). Diet containing 35% crude protein improves energy balance, growth, and feed conversion in the Amazon river prawn, Macrobrachium amazonicum. *Aquaculture Reports*, *21*, 100962. https://doi.org/10.1016/j.aqrep.2021.100962
33. Markweg-Hanke, M., Lang, S., & Wagner, F. (1995). Dodecanoic acid inhibition of a lipase from Acinetobacter sp. OPA 55. *Enzyme and Microbial Technology*, *17*(6), 512. https://doi.org/10.1016/0141-0229(94)00067-2
34. Maschmeyer, T., Luque, R., & Selva, M. (2020). Upgrading of marine (fish and crustaceans) biowaste for high added-value molecules and bio (nano)-materials. *Chemical Society Reviews*, *49*, 4527.
35. Mohan, K., Rajan, D. K., Muralisankar, T., Ganesan, A. R., Sathishkumar, P., & Revathi, N. (2022). Use of black soldier fly (Hermetia illucens L.) larvae meal in aquafeeds for a sustainable aquaculture industry: A review of past and future needs [Review of *Use of black soldier fly (Hermetia illucens L.) larvae meal in aquafeeds for a sustainable aquaculture industry: A review of past and future needs*]. *Aquaculture*, *553*, 738095. Elsevier BV. https://doi.org/10.1016/j.aquaculture.2022.738095
36. Moutinho, S., Oliva-Teles, A., Martínez-Llorens, S., Monroig, Ó., & Perés, H. (2022). Total fishmeal replacement by defattedHermetia illucens larvae meal in diets for gilthead seabream (Sparus aurata) juveniles. *Journal of Insects as Food and Feed*, *8*(12), 1455. https://doi.org/10.3920/jiff2021.0195
37. Nairuti, R. N., Musyoka, S. N., Yegon, M. J., & Opiyo, M. A. (2021). Utilization of Black Soldier Fly (Hermetia illucens Linnaeus) Larvae as a Protein Source for Fish Feed: A Review [Review of *Utilization of Black Soldier Fly (Hermetia illucens Linnaeus) Larvae as a Protein Source for Fish Feed: A Review*]. *Aquaculture Studies*, *22*(2). https://doi.org/10.4194/aquast697
38. Peng, K., Chen, X., Lü, H., Zhao, J., Chen, Y., Li, C., Huo, L., & Huang, W. (2022). Effect of dietary soybean meal on growth performance, apparent digestibility, intestinal digestive enzyme activity and muscle growth-related gene expression of Litopenaeus vannamei. *Frontiers in Marine Science*, *9*. https://doi.org/10.3389/fmars.2022.945417
39. Peng, K., Qiu, J., Li, C., Lü, H., Liu, Z., Liu, D., & Huang, W. (2023). A multi-angle analysis of injury induced by supplementation of soybean meal in Litopenaeus vannamei diets. *Frontiers in Microbiomes*, *2*. https://doi.org/10.3389/frmbi.2023.1113635
40. Riolo, K., Rotondo, A., Torre, G. L. L., Marino, Y., Franco, G. A., Crupi, R., Fusco, R., Paola, R. D., Oliva, S., Marco, G. D., Savastano, D., Cuzzocrea, S., Gugliandolo, E., & Giannetto, A. (2023). Cytoprotective and Antioxidant Effects of Hydrolysates from Black Soldier Fly (Hermetia illucens). *Antioxidants*, *12*(2), 519. https://doi.org/10.3390/antiox12020519
41. Secci, G., Mancini, S., Iaconisi, V., Gasco, L., Basto, A., & Parisi, G. (2018). Can the inclusion of black soldier fly (Hermetia illucens) in diet affect the flesh quality/nutritional traits of rainbow trout (Oncorhynchus mykiss) after freezing and cooking? *International Journal of Food Sciences and Nutrition*, *70*(2), 161. https://doi.org/10.1080/09637486.2018.1489529
42. Sha, H., Lü, J., Chen, J., & Xiong, J. (2024). Rationally designed probiotics prevent shrimp white feces syndrome via the probiotics–gut microbiome–immunity axis. *Npj Biofilms and Microbiomes*, *10*(1). https://doi.org/10.1038/s41522-024-00509-5

43. S.T., I., & Belsare, S. G. (2021). Evaluation of some formulated diets for rearing the post-larvae of Macrobrachium rosenbergii. *AquaDocs (United Nations Educational, Scientific and Cultural Organization)*. http://hdl.handle.net/1834/32438
44. Sun, C., Liu, B., Zhou, Q., Xiong, Z., Shan, F., & Zhang, H. (2020). Response of Macrobrachium rosenbergii to Vegetable Oils Replacing Dietary Fish Oil: Insights From Antioxidant Defense. *Frontiers in Physiology*, *11*. https://doi.org/10.3389/fphys.2020.00218
45. Susilo, U., & Rachmawati, F. N. (2020). Protease, Lipase and Amylase Activities in Barred Loach, Nemacheilus Fasciatus C.V. *Jurnal Biodjati*, *5*(1), 115. https://doi.org/10.15575/biodjati.v5i1.6530
46. Tayyab, M., Zhao, Y., & Zhang, Y. (2025). Microbiome engineering to enhance disease resistance in aquaculture: current strategies and future directions [Review of *Microbiome engineering to enhance disease resistance in aquaculture: current strategies and future directions*]. *Frontiers in Microbiology*, *16*. Frontiers Media. https://doi.org/10.3389/fmicb.2025.1625265
47. Valente, C. de S., Coates, C. J., Cagol, L., Bombardelli, R. A., Becker, A. G., Schmidt, D., Heinzmann, B. M., Santos, A. M. V. dos, Baldisserotto, B., & Ballester, E. L. C. (2024). Antioxidant status and performance of Macrobrachium rosenbergii juveniles fed diets containing non-nutritive Aloysia triphylla essential oil. *Aquaculture International*, *32*(6), 7201. https://doi.org/10.1007/s10499-024-01509-0
48. Vieira, S. A., Zhang, G., & Decker, E. A. (2017). Biological Implications of Lipid Oxidation Products. *Journal of the American Oil Chemists Society*, *94*(3), 339. https://doi.org/10.1007/s11746-017-2958-2
49. Wang, G., Peng, K., Hu, J., Mo, W., Wei, Z., & Huang, Y. (2021). Evaluation of defatted Hermetia illucens larvae meal for Litopenaeus vannamei : effects on growth performance, nutrition retention, antioxidant and immune response, digestive enzyme activity and hepatic morphology. *Aquaculture Nutrition*, *27*(4), 986. https://doi.org/10.1111/anu.13240
50. Wang, Q., Qi, Z., Fu, W., Pan, M., Ren, X., Zhang, X., & Rao, Z. (2024). Research and Prospects of Enzymatic Hydrolysis and Microbial Fermentation Technologies in Protein Raw Materials for Aquatic Feed. *Fermentation*, *10*(12), 648. https://doi.org/10.3390/fermentation10120648
51. Wiszniewski, G., Jarmołowicz, S., Hassaan, M. S., Mohammady, E. Y., Soaudy, M. R., Łuczyńska, J., Tońska, E., Terech-Majewska, E., Ostaszewska, T., Kamaszewski, M., Skrobisz, M., Adamski, A., Schulz, P., Kaczorek-Łukowska, E., & Siwicki, A. K. (2019). The use of bromelain as a feed additive in fish diets: Growth performance, intestinal morphology, digestive enzyme and immune response of juvenile Sterlet (Acipenser ruthenus). *Aquaculture Nutrition*, *25*(6), 1289. https://doi.org/10.1111/anu.12949
52. Xie, J., Xie, W., Yu, J., Xin, R., Shi, Z., Song, L., & Yang, X. (2021). Extraction of Chitin From Shrimp Shell by Successive Two-Step Fermentation of Exiguobacterium profundum and Lactobacillus acidophilus. *Frontiers in Microbiology*, *12*. https://doi.org/10.3389/fmicb.2021.677126
53. Yan, Y., Sun, Y., Cui, J., Gao, J., Chai, Y., & Liu, Z. (2025). Environmental factors and microbial interactions drive microbial community succession during solid-state fermentation of corn husk for microbial biomass protein production. *Frontiers in Microbiology*, *16*. https://doi.org/10.3389/fmicb.2025.1646555
54. Yang, Y., Zhu, T., Jin, M., Li, X., Xie, S., Cui, Y., & Zhou, Q. (2025). Black soldier fly larvae oil can partially replace fish oil in the diet of the juvenile mud crab (Scylla paramamosain). *Animal Nutrition*, *20*, 469. https://doi.org/10.1016/j.aninu.2025.01.002
55. Yohana, M. A., Ray, G. W., Yang, Q., BeiPing, T., Chi, S., & Deng, J. (2023). Effect of soybean meal replacement with corn gluten meal on the survival, biochemical and metabolic responses, and disease resistance of Pacific white shrimp (Litopenaeus vannamei). *Annals of Animal Science*, *24*(2), 575. https://doi.org/10.2478/aoas-2023-0085
56. Zainab-L, I., Ng, W., & Sudesh, K. (2022). Potential of mealworms used in polyhydroxyalkanoate/bioplastic recovery as red hybrid tilapia (Oreochromis sp.) feed ingredient. *Scientific Reports*, *12*(1). https://doi.org/10.1038/s41598-022-13429-1
57. Zhang, Y., Ishikawa, M., Koshio, S., Yokoyama, S., Dossou, S., Wang, W., Zhang, X., Shadrack, R. S., Mzengereza, K., Zhu, K., & Seo, S. (2021). Optimization of Soybean Meal Fermentation for Aqua-Feed with Bacillus subtilis natto Using the Response Surface Methodology. *Fermentation*, *7*(4), 306. https://doi.org/10.3390/fermentation7040306